A simulated soil moisture based drought analysis for the United States

Justin Sheffield,[1] Gopi Goteti,[2] Fenghua Wen,[3] and Eric F. Wood[1]

Received 30 June 2004; revised 7 October 2004; accepted 25 October 2004; published 29 December 2004.

[1] Droughts have severe economic, environmental and social impacts. Timely determination of the current level of drought may aid the decision making process in reducing the impacts from drought. In this study, high-resolution, land surface hydrology simulations using the Variable Infiltration Capacity (VIC) model are used to derive a hydrologically based drought index. Soil moisture data from a retrospective simulation from 1950 to 1999 over the continental United States are used to develop probability distributions of monthly average soil moisture, and the relative position of soil moisture fields within the historic distribution provides a measure of drought in relation to the long-term behavior. The index is able to identify the major drought events during the latter part of the twentieth century and shows good agreement with the time series of U.S. drought from two Palmer Drought Severity Index (PDSI) data sets. On average, 30% of the United States experienced dry conditions (<10% soil moisture quantile) during 1950–1999, peaking at over 70% coverage at the height of the 1950s drought. Many dry events exhibit long-term persistence, especially in the West, which is important in terms of the cumulative impacts. The physical basis of the model allows the index to take into account a number of processes, which contribute to the development of drought, such as snow accumulation and melt that other indices ignore or treat unsatisfactorily. Furthermore, the high spatial and temporal resolution of the simulations ensure that the drought index is able to allow for the effects of short-term changes in meteorology as well as longer-term climate variations, and resolve the high spatial variability in soil moisture and drought occurrence. The potential for implementing the analysis in an operational mode exists by using data from the near real-time simulations within the North American Land Data Assimilation System (NLDAS). *INDEX TERMS:* 1812 Hydrology: Drought; 1866 Hydrology: Soil moisture; 1833 Hydrology: Hydroclimatology; *KEYWORDS:* drought, soil moisture, United States

Citation: Sheffield, J., G. Goteti, F. Wen, and E. F. Wood (2004), A simulated soil moisture based drought analysis for the United States, *J. Geophys. Res.*, *109*, D24108, doi:10.1029/2004JD005182.

1. Introduction

[2] Droughts in the United States result in an estimated average annual damage of U.S.$6–8 billion [*Wilhite*, 2000]. The estimated loss from the 1988 drought was U.S.$40 billion [*American Meteorological Society*, 1997] and the estimated loss for the state of Texas alone from the 1996 drought was U.S.$6 billion [*Wilhite*, 2000]. In order to mitigate the losses caused by droughts and to plan and manage the water shortages that will accompany future droughts, it is necessary to develop scientifically based drought monitoring tools and warning systems. Such tools can be used to make quantitative measures of drought characteristics, enabling the transfer of these measures from one region to the other. One of the most widely used measures of drought is the *Palmer* [1965] index, and is used by agencies such as the National Weather Service's Climate Prediction Center (CPC). Other measures of drought, such as the Standardized Precipitation Index [*McKee et al.*, 1993, 1995], and the satellite based vegetation and temperature condition index [*Kogan*, 1997] are also in use. The Drought Monitor [*Svoboda et al.*, 2002] is a recent initiative to combine a number of different indices into a consistent national indicator. A description of the drought measures developed over the last century can be found in *Heim* [2002].

[3] Depending upon the nature of the water deficit and the objectives of its use, several definitions of drought have come into existence [see, e.g., *American Meteorological Society*, 1997; *Dracup et al.*, 1980; *Heim*, 2002; *Palmer*, 1965; *Rasmussen et al.*, 1993]. In the scientific literature, droughts are typically classified into four major types: (1) meteorological drought: usually defined as a significant negative deviation from mean precipitation; (2) hydrological drought: a deficit in the supply of surface and subsurface water; (3) agricultural drought: a combination of meteoro-

[1]Department of Civil and Environmental Engineering, Princeton University, Princeton, New Jersey, USA.
[2]Department of Earth System Science, University of California, Irvine, California, USA.
[3]Department of Mathematics, New York University, New York, USA.

Copyright 2004 by the American Geophysical Union.
0148-0227/04/2004JD005182

logical and hydrological droughts resulting in reduced supply of moisture for crops; and (4) socioeconomic drought: a combination of the above three droughts leading to undesirable social and economic impacts. The above classification of droughts is not rigid since the definitions incorporate many different physical, biological and socioeconomic variables. Moreover, droughts of the same type can differ from each other in their intensity, duration and spatial coverage.

[4] Each of the standard indices in operational use has its advantages and disadvantages [e.g., *Keyantash and Dracup*, 2002]. While the Drought Monitor attempts to provide a consistent and useable product it may suffer from the inadequacies of the contributing indices. The development of drought is a complex process that depends on a variety of factors [*Wilhite*, 2000]. It therefore may be necessary to include as many of the contributing processes as possible when trying to derive an accurate drought index that can be used consistently over a region for a variety of applications. For example, agricultural drought is not only dependent on the temporal availability of precipitation and soil moisture for replacement of evapotranspiration losses but also depends on the vertical distribution of soil moisture that is available to plants at different phenological stages of development. Soil moisture profiles, although correlated with precipitation at monthly timescales, can show very nonlinear responses to precipitation at shorter timescales, especially at lower depths and with dry initial conditions [e.g., *Capehart and Carlson*, 1997]. Additionally, in regions that experience substantial snowfall, the accumulation of the snow pack in the winter and the subsequent melt during the spring may be a major contributing factor to spring/summer drought occurrence [*Service*, 2004]. To determine the occurrence and intensity of drought in such regions, one has to take into account these complex processes.

[5] Observations of hydrologic variables and processes are scarce over the large spatial scales that are of interest in drought monitoring and mitigation strategies. Precipitation is one of the best observed variables although observations may be limited in spatial and temporal coverage, especially over sparsely populated regions and complex terrain. Soil moisture is one of the least observed aspects of the hydrologic cycle in terms of long-term, large-scale measurements. Because of the lack of large scale and long term observations of soil moisture in the United States and elsewhere, the use of simulated soil moisture fields from land surface models forced with observed precipitation and near surface meteorology is a viable alternative. Some of the standard drought indices rely on some form of modeling and take into account hydrological processes to some degree, but the simplifications and assumptions used may result in an inadequate representation of drought. This is especially the case in regions whose hydrology is more complex, for example in cold regions and over varied terrain. For example, the PDSI calculates water balance terms when estimating cumulative moisture deficits. However, it is limited in its widespread application because of its empirical nature and U.S. agricultural basis, and incorporates a number of simplifications, such as its simple water balance model and inadequate handling of frozen precipitation [*Alley*, 1984; *Heim*, 2002].

[6] In recent years, the development and use of land surface modeling schemes has increased as the central role of the land surface within the climate/weather system has gained acceptance [*Entekhabi et al.*, 1996; *Koster et al.*, 2003]. State of the art schemes model a multitude of processes, including cold season effects, vegetation development and full energy partitioning and do this using a variety of advanced techniques including multilayer soil models with full water and energy accounting and subgrid variability of hydrological processes. By modeling the transport and storage of water in detail these schemes are highly suited to the analysis of the occurrence and intensity of drought and can do this on time and space scales that are useful in a wide variety of impacts and applications. However, the lack of consistent high-resolution meteorological forcing data required by these models has prevented their operational use in the past. Now with the advent of high computational power and the availability of observational data via telemetry and remote sensing and modeled meteorological data sets from atmospheric forecast models, it is now feasible to generate operational land surface hydrological data products over large scales [e.g., *Mitchell et al.*, 2004], which can in turn provide the capability for operational drought monitoring. The use of modeling also provides the potential for drought forecasting using seasonal forecasts from coupled ocean-atmosphere general circulation models.

[7] *Heim* [2002] details the currently available drought indices for the United States but notes that, despite considerable progress being made (e.g., the Drought Monitor), there are still improvements to be made. These include, incorporating additional indicators such as snowpack data, reservoir and groundwater levels, and the daily variability of precipitation occurrence. Furthermore, Heim suggests the following characteristics are necessary for operational drought monitoring: (1) availability of data on a near real-time basis; (2) national coverage; (3) complete historical data sets to form a basis for comparison; and (4) removal of nonclimatic biases.

[8] In this study, we develop a hydrologically based drought analysis for the United States that attempts to address some of these issues. The analysis is based on soil moisture derived from high-resolution, long-term retrospective and near real-time simulations of the land surface water and energy budgets. Monthly statistical distributions for soil moisture are developed for each model grid cell, and drought severity is represented as quantiles of the soil moisture distribution. These data products provide the opportunity to develop a drought analysis and real-time monitoring system based on physical quantities and processes that reflect the causes and impacts of drought.

2. Soil Moisture Data

[9] Soil moisture is a good index of drought, reflecting recent precipitation and antecedent conditions and indicating agricultural potential and available water storage [*Keyantash and Dracup*, 2002]. The soil column acts as a filter between incoming precipitation and throughfall (direct precipitation plus canopy drainage) and processes that remove water from the hydrologic system, i.e., evapotranspiration and subsurface drainage [*Entekhabi et al.*, 1996]. The amount

21562202d, 2004, D24, Downloaded from https://agupubs.onlinelibrary.wiley.com/doi/10.1029/2004JD005182, Wiley Online Library on [24/05/2023]. See the Terms and Conditions (https://onlinelibrary.wiley.com/terms-and-conditions) on Wiley Online Library for rules of use; OA articles are governed by the applicable Creative Commons License

of water in the top layers of the soil is correlated with short-term precipitation and meteorology and gives a measure of meteorological drought. The soil moisture in the root zone is a governing factor of the state of vegetative growth through the availability of water for transpiration and thus is a direct indicator of agricultural drought [*Keyantash and Dracup*, 2002]. In deeper soil layers, the soil moisture levels and depth to ground water reflect long-term or hydrological drought as it is this water that is available for recharge to aquifers and rivers.

[10] The soil moisture data used in this study are derived from simulations using the Variable Infiltration Capacity (VIC) land surface hydrology model. The simulations were carried out as part of the North American Land Data Assimilation System (NLDAS) [*Maurer et al.*, 2002; *Mitchell et al.*, 1999, 2000, 2004], which is a multi-institution project that attempts to provide land surface states for assimilation into weather prediction schemes for improved forecasts. The modeling domain is a regular 1/8th degree grid over the continental United States. Data from a retrospective simulation provide a climatology against which the state of drought at any chosen time can be deduced. Data are also available from near real-time simulations.

2.1. Variable Infiltration Capacity (VIC) Model

[11] The VIC macro-scale energy and water balance model has been developed over the last 10 years at the University of Washington and Princeton University. The distinguishing features of the VIC land surface hydrology model [*Liang et al.*, 1994, 1996; *Cherkauer et al.*, 2002], compared to other soil-vegetation-atmosphere transfer schemes (SVATS), are the representation of subgrid variability in soil storage capacity as a spatial probability distribution, and the parameterization of baseflow as a nonlinear recession from the lower soil moisture zone [*Dumenil and Todini*, 1992]. The VIC model has been tested and applied at a range of scales, from small river basins to continental and global scales [see, e.g., *Abdulla et al.*, 1996; *Nijssen et al.*, 1997, 2001]. The land surface is represented by a specified number of tiled land cover classes and the subsurface is discretized into a number of soil layers. Movement of moisture between the soil layers is modeled as gravity drainage, with the unsaturated hydraulic conductivity a function of the degree of saturation of the soil [*Campbell*, 1974]. Three soil layers were used in the NLDAS simulations with the top layer being 10 cm deep. The depth of the second layer, the main storage layer, varies between 0.5 and 1.5 m over the modeling domain. The lower layer, which provides moisture for subsurface runoff, is typically between 0.1m and 0.25m. The depths of these two lower layers are adjusted during the calibration process to result in runoff fluxes that satisfactorily match large basin streamflow measurements.

2.2. Fifty-Year Retrospective Simulation

[12] *Maurer et al.* [2002] simulated the land surface water budget of the contiguous United States with the VIC model for the period 1950–99 at 1/8th degree and 3-hourly resolution over the NLDAS modeling grid. Soil moisture states from this simulation are used as the background climatology for the drought index. Meteorological forcings for the simulation are based on observed station data for precipitation and temperature. The other required variables, vapor pressure, incoming longwave and shortwave radiation and air pressure, were derived using predictive relationships with daily precipitation and diurnal temperature range. Wind speed was taken from the National Centers for Environmental Prediction and National Center for Atmospheric Research (NCEP/NCAR) reanalysis. Precipitation daily totals were derived from the National Oceanic and Atmospheric Administration (NOAA) Cooperative Observer (Co-op) stations and gridded at 1/8th degree resolution and then scaled to match the Parameter-elevation Regressions on Independent Slopes Model (PRISM) long-term averages. Minimum and maximum daily temperatures were also obtained from the Co-op stations and similarly gridded and adjusted for the elevation of the grid using the environmental lapse rate. Daily precipitation totals were apportioned evenly within each 3-hourly time step. The diurnal cycle of temperature was generated by spline fitting to the daily maximum and minimum values.

[13] Although simulated soil moisture fields are potential surrogates for actual observations and are indeed the only viable alternative over large scales, their accuracy must be sufficient to instill confidence in their use. *Maurer et al.* [2001, 2002] obtained good comparisons of the retrospective simulation soil moisture and other hydrologic variables with observations. Comparison of soil moisture states with localized measurements from the Illinois soil moisture network showed that the VIC simulation captured the changes in soil moisture and inter-annual variability and the soil moisture persistence well. Simulated interannual variability in streamflow and peak and low flows showed good agreement with naturalized streamflow records. Radiation fluxes were compared with measurements from a number of Surface Radiation Budget Network (SURFRAD) energy flux measurement sites [*Augustine et al.*, 2000] across the United States and showed reasonable agreement for daily fluxes and some underestimation of peak flux. For cold season processes, simulated snow cover extent matched well the National Snow and Ice Data Center (NSIDC) Northern Hemisphere snow extent data set although there was some underestimation in the northern Great Plains.

2.3. Real-Time Simulation

[14] Central to the NLDAS is the near real-time implementation of land surface models to produce operational products of land surface fluxes and states. This simulation mode has been in operation since April 1999 and runs daily at a lag of about 12 hours to real time. The real time forcings are obtained from a variety of sources including the NCEP Eta Data Assimilation System (EDAS), the CPC daily gauge-based precipitation analysis, the National Weather Service (NWS) hourly Doppler radar precipitation product, and Geostationary Operational Environmental Satellite (GOES)-based shortwave radiation data [*Cosgrove et al.*, 2003]. These particular forcing products have been obtained back to September 1996 and have been used to force a separate retrospective simulation covering the period September 1996 to September 1999. This 3-year retrospective period has not been used in this study but comparisons were made between the 3-year and the 50-year retrospective to ensure consistency. De-

21562202d, 2004, D24, Downloaded from https://agupubs.onlinelibrary.wiley.com/doi/10.1029/2004JD005182, Wiley Online Library on [24/05/2023]. See the Terms and Conditions (https://onlinelibrary.wiley.com/terms-and-conditions) on Wiley Online Library for rules of use; OA articles are governed by the applicable Creative Commons License

tailed diagnosis of VIC model output has been carried out over the 1996–1999 retrospective period for all aspects of the water and energy cycles in a series of validation studies. Comparisons of soil moisture with the observations from the Oklahoma Mesonet [*Brock et al.*, 1995] showed that VIC was able to simulate the variability in soil moisture [*Robock et al.*, 2003]. *Sheffield et al.* [2003] compared model output with the NOAA Multi-Sensor Snow and Ice Mapping System daily snow cover extent analysis and VIC had reasonable skill in simulating the spatial extent of snow cover and the timing of spring melt over regional scales. The study of *Pan et al.* [2003] compared model output with annual snow water equivalent accumulations from the SNOTEL network [*Crook*, 1977] over the western mountains and showed that VIC was able to simulate the annual accumulation of the snow pack on a regional basis.

3. Methods

[15] The 3-hour soil moisture states from the retrospective simulation were averaged to a monthly time step for the 50-year period (1950–1999). Other time steps, like weekly, could easily be accommodated within the analysis. The statistical moments of the data were calculated and used to fit probability distributions to the data. The VIC drought index for a particular soil moisture value can then be derived as the equivalent quantile of the probability distribution. A detailed description of these methods is given next.

3.1. Empirical Moments of Soil Moisture Variability

[16] The statistical characteristics of hydrologic variables, including soil moisture can be best described by L-moments [*Stedinger et al.*, 1993], which have the theoretical advantage over conventional moments of being more robust to the presence of outliers and are able to characterize a wider range of distributions [*Hosking*, 1990]. L-moments can be written in terms of linear combinations of probability-weighted moments (PWMs). For a set of random variables $X_j(X_1, X_2, \ldots, X_n)$, unbiased estimators for the first three PWMs are

$$b_0 = \overline{X}$$

$$b_1 = \sum_{j=1}^{n-1} \frac{(n-j)X_{(j)}}{n(n-1)} \tag{1}$$

$$b_2 = \sum_{j=1}^{n-2} \frac{(n-j)(n-j-1)X_{(j)}}{n(n-1)(n-2)}$$

The L-moments are calculated in terms of PWMs and are defined as

$$\lambda_1 = b_0 \tag{2}$$

$$\lambda_2 = 2b_1 - b_0 \tag{3}$$

$$\lambda_3 = 6b_2 - 6b_1 + b_0 \tag{4}$$

The sample estimates using the L-moments are defined as

$$L_{mean}(\mu_s) = \lambda_1 \tag{5}$$

$$L_{CV}(\sigma_s/\mu_s) = \frac{\lambda_2}{\lambda_1} \tag{6}$$

$$L_{skew}(\gamma_s) = \frac{\lambda_3}{\lambda_2} \tag{7}$$

3.2. Soil Moisture Probability Distributions

[17] The drought index is based on the cumulative probability of soil moisture fitted to the simulated soil moisture values. Given the magnitude and variability of the distribution of the sample estimates, and the different signs assumed by the L_{skew} coefficient, the Beta probability distribution function (PDF) was chosen to represent the monthly distribution of soil moisture. The Beta distribution can assume a wide variety of shapes and is flexible enough to account for positive and negative values of L_{skew}. A generalized form of the Beta distribution, defined on limits a and b, with $a < b$, is of the form:

$$f(\theta) = \frac{1}{B(b-a)^{t-1}}(\theta - a)^{r-1}(b-\theta)^{t-r-1}, \qquad \text{where } a \le \theta \le b \tag{8}$$

where θ is the volumetric soil moisture content; $r > 0$ and $t > r$ are constraints on the distribution shape parameters; and $B = \Gamma(r)\,\Gamma(t-r)/\Gamma(t)$. The usual form of the Beta distribution has $a = 0$ and $b = 1$. The parameter b represents the upper limit on soil moisture and is a function of soil porosity, which is in the range 30–60% by volume. The parameter a represents the lower limit, which is related to soil properties and climatic factors. The parameters r and t do not have any direct physical significance but determine the shape of the distribution and its moments.

[18] The parameters a, b, r and t were estimated for each grid location. Parameter $a(b)$ was estimated by assuming that the first (last) 10% of the sorted soil moisture values are linearly related to its empirical cumulative distribution function. To determine r and t, once a and b were estimated, the sample estimators from the L-moments were equated to the corresponding distribution parameters. In theory, any of the two moments can be used to estimate r and t. In practice, it was found that if the first two moments were used, the resulting skew coefficient using the estimated parameters fit poorly the empirical skew coefficient (not shown). An alternative approach, which is recognized as akin to model calibration, is to use all three empirical L-moments to estimate r and t, resulting in a system of three simultaneous equations to estimate two unknowns (r, t). A "best-fit" solution for r and t was found by minimizing the objective function:

$$\text{error} = \frac{(\mu - \mu_s)^2}{\mu_s^2} + \frac{\left(\sigma^2 - \sigma_s^2\right)^2}{\left(\sigma_s^2\right)^2} + \frac{(\gamma - \gamma_s)^2}{\gamma_s^2} \tag{9}$$

using the shuffled complex evolution global optimization algorithm (SCE-UA) of *Duan et al.* [1992, 1993, 1994].

21562202d, 2004, D24, Downloaded from https://agupubs.onlinelibrary.wiley.com/doi/10.1029/2004JD005182, Wiley Online Library on [24/05/2023]. See the Terms and Conditions (https://onlinelibrary.wiley.com/terms-and-conditions) on Wiley Online Library for rules of use; OA articles are governed by the applicable Creative Commons License

21562202d, 2004, D24, Downloaded from https://agupubs.onlinelibrary.wiley.com/doi/10.1029/2004JD005182, Wiley Online Library on [24/05/2023]. See the Terms and Conditions (https://onlinelibrary.wiley.com/terms-and-conditions) on Wiley Online Library for rules of use; OA articles are governed by the applicable Creative Commons License

[19] To test the goodness-of-fit of the Beta distribution, the Kolmogorov-Smirnov (KS) nonparametric test was used. The KS test statistic, for a set of ranked soil moisture values, is defined as the absolute maximum value of D obtained from the following equation:

$$D = G(\theta) - q(\theta) \tag{10}$$

where $G(\theta)$ is the empirical cumulative probability estimated as $G(\theta) - i/N$; where θ is the ith smallest value in the set of sorted soil moisture values; and $q(\theta)$ is the theoretical cumulative probability given by equation (11). The null hypothesis that the soil moisture data were sampled from a Beta distribution is rejected for values of D that exceed a critical value at the 95% significance level. Although the KS statistic is the least discriminating test available, it is appropriate to use it here as it is an exact test and is independent of the underlying cumulative distribution function.

3.3. Calculation of the Drought Index

[20] Equation (8) was used to estimate the PDF of monthly soil moisture, for each month. The VIC drought index is represented by the quantile $q(\theta)$ corresponding to a soil moisture value θ, and is determined by integrating the PDF over (a, θ). The integral of the PDF is approximated to a summation (equation (11)) and is used to derive spatial fields of the drought index.

$$q(\theta) = \int_a^{\theta} f(\theta)d\theta \approx \sum_{i=1}^{i=M} f(a + (i-1) * \Delta\theta + \Delta\theta/2) * \Delta\theta \tag{11}$$

where $a \leq \theta \leq b$, M is a large integer (1000 in this study), and $\Delta\theta = (\theta - a)/M$.

4. Results and Analysis

4.1. Soil Moisture Variability

[21] The sample estimates of fractional soil moisture content using L-moments, namely, the mean (L_{mean}), coefficient of variation (L_{CV}) and skewness (L_{skew}), for the total soil column are shown in Figure 1 for July. It should be emphasized that these maps are derived for fractional and not absolute water content and so show amount of water relative to the local soil capacity. In general, the west and Midwest are relatively drier than the central and eastern United States, which reflects the precipitation gradient across the country. Within this pattern, there are distinct wet and dry regions. Notably, there are wetter regions along the Pacific coast, western Cascades and the western edge of the Sierra Nevada during the winter. These recede to the Pacific coast of Oregon and Washington State and the central Cascade Range and Sierra Nevada during the summer. Other wet regions exist over the Rockies, markedly during the summer after spring snowmelt, in central Idaho, northeast Montana and also in northeast Wyoming and Colorado. In the east, relatively wetter conditions exist through the lower Mississippi and Ohio River basins with wetter conditions experienced in the winter, reflecting the lower evaporation in this season. Relatively dry regions occur in the lee of the Cascades in eastern Washington State, eastern Oregon through into southern Idaho and also in the desert regions of the southwest that are characterized by low precipitation and high potential evaporation.

[22] The low values of L_{CV} suggest that the annual variation of monthly soil moisture is not large, and that, in absolute terms, the extreme values of soil moisture lie near the mean value. Low L_{CV} values appear through the mid- Mississippi basin and up into the Ohio basin and at scattered locations through the West. In general, regions of higher variation occur along the eastern side of the Appalachian chain and down into Florida, possibly due to the wetter climate and sandier soils, and in scattered patterns across the western side of the country. A number of regions of high variation stand out, such as in southeast Idaho, southeast California and Arizona, northwest New Mexico, and in eastern and southernmost Texas. These regions are affected by the El Nino-Southern Oscillation (ENSO), which may account for much of this variability [*Piechota and Dracup*, 1996; *Rajagopalan et al.*, 2000]. The L_{skew} statistic takes on both positive and negative values. During winter, negative values are apparent along the Pacific coast and over the Mississippi and Ohio basins. Positive values, which indicate a tendency toward dry soil moisture values, appear over the Midwest and West and up from Florida along the eastern seaboard. During the summer most of the arid regions in the western half of United States exhibit a positive skew due to being influenced by ENSO and the North American monsoon, and the majority of the wetter eastern portion of the United States show a negative skew.

4.2. Soil Moisture Probability Density Functions (PDF) and Drought Quantiles

[23] PDFs of soil moisture were generated for each 1/8th degree model grid cell over the conterminous United States using the 50-year retrospective simulation. The Kolmogorov-Smirnov (K-S) statistic (equation (10)) was used to assess the accuracy of the fit of the PDF to the data. Figure 2 shows the estimated parameters (a, b, r and t) of the PDFs. Figure 3 shows examples of the fitted PDFs for four model grid cells located in different climate zones across the United States. The monthly time series of 10% and 90% quantiles of soil moisture obtained using equation (11) are also shown in Figure 3 for these grid cells. Drought index values can be derived for a given volumetric soil moisture value at any point in the domain by integrating the PDF up to this value (equation (11)). Very different behavior is evident among the four example grid cells, in terms of distribution mean and shape, and in seasonal variation, ranging from high fractional soil moisture values and considerable seasonality in the northwest (grid cell 1, western foothills of the Cascade Range in Washington state), to relatively low fractional soil moisture values and essentially no seasonal cycle in southeast California (grid cell 4, located in the Mojave Desert).

4.3. Drought Occurrence Over the Last 50 Years

4.3.1. National Scale

[24] Figure 4 shows the time series of monthly VIC drought index averaged over the United States from 1950 to 1999. Also shown is the monthly time series of the percentage area of the United States that is experiencing severe drought conditions, where a severe drought is de-

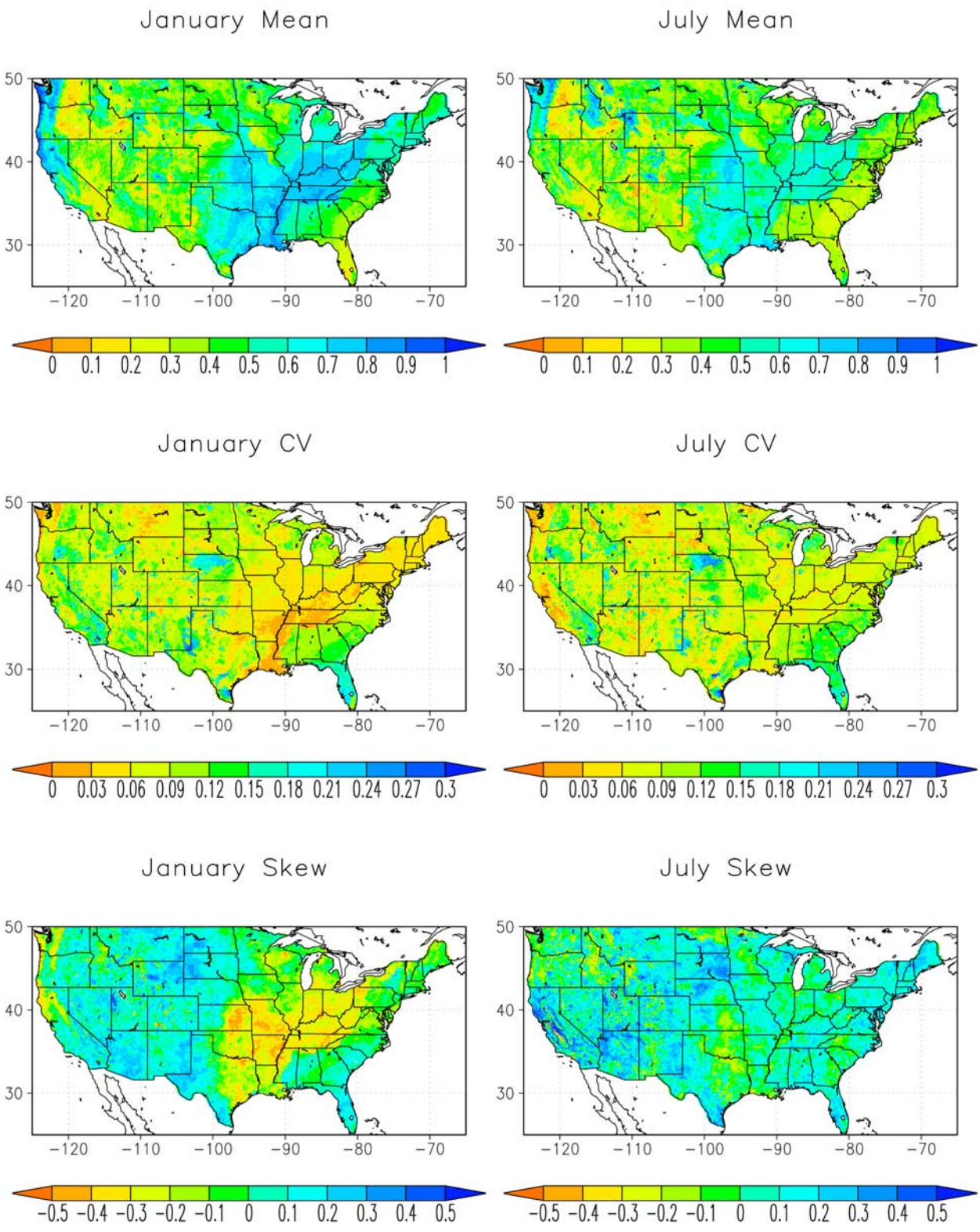

Figure 1. Sample L-moment statistics (mean, CV, and skew) of the monthly average fractional soil moisture from the VIC 50-year (1950–1999) retrospective simulation for July.

fined here as an index value less than 10%. The United States has undergone a number of major droughts during the last 50 years, many of which have been severe in terms of their impacts to agriculture and society. A number of significant dry events can be identified in the time series of average values that correspond to these major historic events. For example, the mid 1950s shows a dry spell (low index values) spanning a number of years which reflects the

21562202d, 2004, D24, Downloaded from https://agupubs.onlinelibrary.wiley.com/doi/10.1029/2004JD005182, Wiley Online Library on [24/05/2023]. See the Terms and Conditions (https://onlinelibrary.wiley.com/terms-and-conditions) on Wiley Online Library for rules of use; OA articles are governed by the applicable Creative Commons License

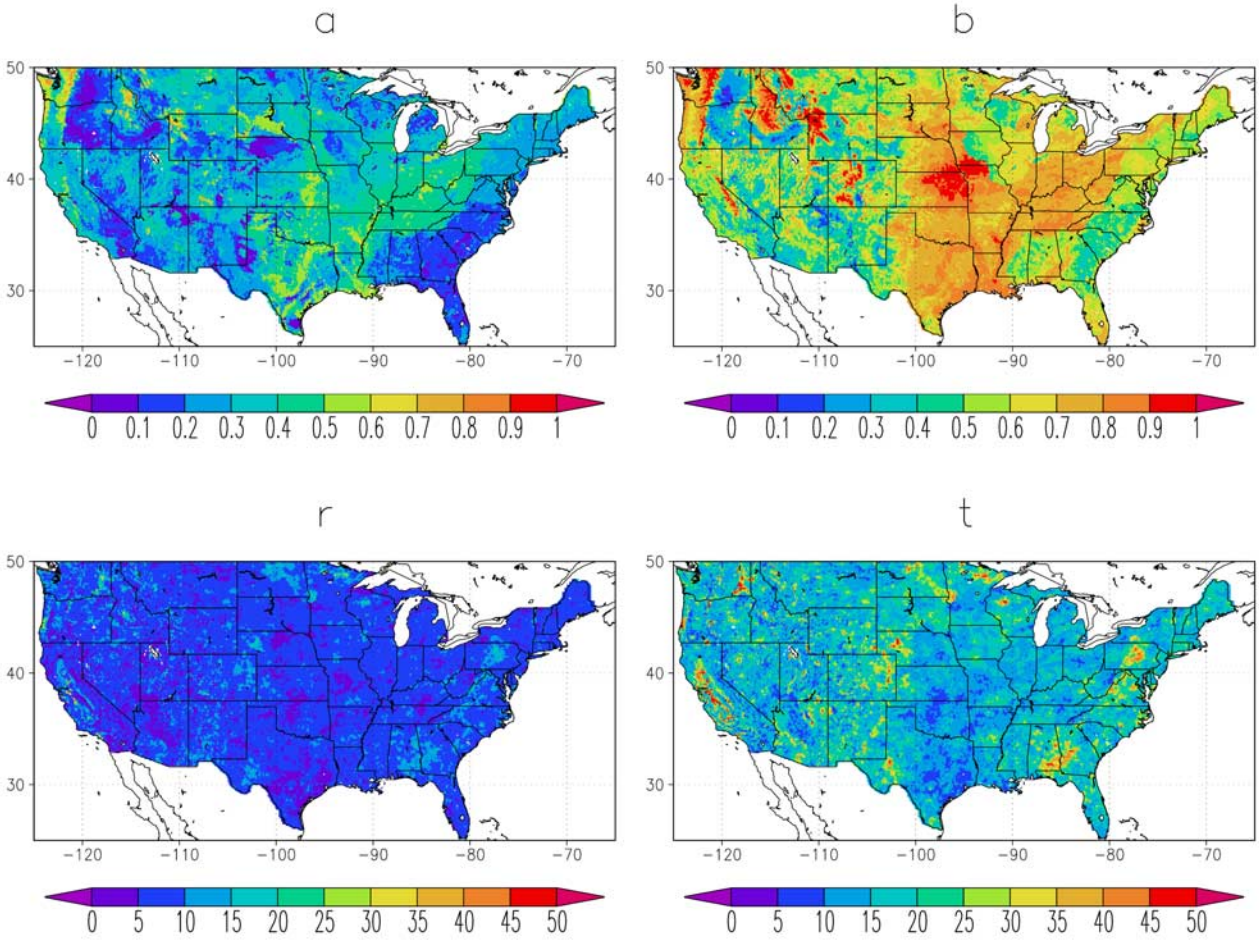

Figure 2. Parameters (a, b, r, t) of the Beta distribution as fitted to the monthly average fractional soil moisture from the VIC 50-year (1950–1999) retrospective simulation. The distributions are fitted using the SCE-UA algorithm and are shown here for July.

long period of drought that occurred in the southwest [*Namias*, 1982; *Diaz*, 1983; *Barlow et al.*, 2001; *Schubert et al.*, 2004] and, most notably, in Texas from 1951 to 1956 [*Diaz*, 1983]. Two moderate events are apparent during the 1960s [*Namias*, 1966, 1967; *Diaz*, 1983; *Barlow et al.*, 2001], which correspond to the drought conditions in the Midwest [*Diaz*, 1983] and northeast [*Namias*, 1966, 1967; *Diaz*, 1983]. During 1987–88, there is a dry period that is consistent with the short term drought conditions that affected a large area of the country, peaking in the spring and summer of 1988 [*Namias*, 1991; *Mo et al.*, 1991; *Trenberth and Branstator*, 1992; *Lyon and Dole*, 1995; *Sud et al.*, 2003]. The time series of the percentage area affected by severe drought conditions (<10% quantile) highlights the extent of these significant events. A number of time periods can be identified that show peaks in the percentage area undergoing such drought: the mid 1950s, the mid 1960s, mid to late 1970s and the late 1980s. The maximum total area of the United States affected during the drought of the 1950s was 63.6% in October 1953, although there are similarly high values in August 1954 (56.0% areal extent), January 1956 (59.6%) and October 1956 (62.6%), with values consistently greater than 40% during 1953–57. A significant peak in February 1977 (68.3% areal extent) is coincident with the moderate drought of 1976–77 which mostly affected the western third of the United States throughout this period and the north-central states during the spring of 1977 [*Diaz*, 1983]. For the drought of 1988–89, the peak extent during June 1988 is 62.9%, but as with the 1977 drought the duration of the event was small compared with the 1950s drought, although the impacts were significant [*Trenberth and Branstator*, 1992]. On average, 30.9% of the United States was under severe (<10% quantile) drought conditions over the period 1950–1999.

4.3.2. Regional Scale

[25] The size and climate diversity of the United States ensures that the spatial variability of drought conditions is high. The time series in Figure 4 shows the general picture of national drought over the past 50 years but does not give much information about where and to what extent drought has occurred across the country. Figure 5 shows time series of the VIC drought index averaged over each of the twelve continental U.S. NWS Regional Forecast Center (RFC) regions for 1950–1999. The monthly variation of drought level is quite different between regions, indicating the high short-term spatial variation in drought occurrence. However, there is a

215622024, 2004, D24, Downloaded from https://agupubs.onlinelibrary.wiley.com/doi/10.1029/2004JD005182, Wiley Online Library on [24/05/2023]. See the Terms and Conditions (https://onlinelibrary.wiley.com/terms-and-conditions) on Wiley Online Library for rules of use; OA articles are governed by the applicable Creative Commons License

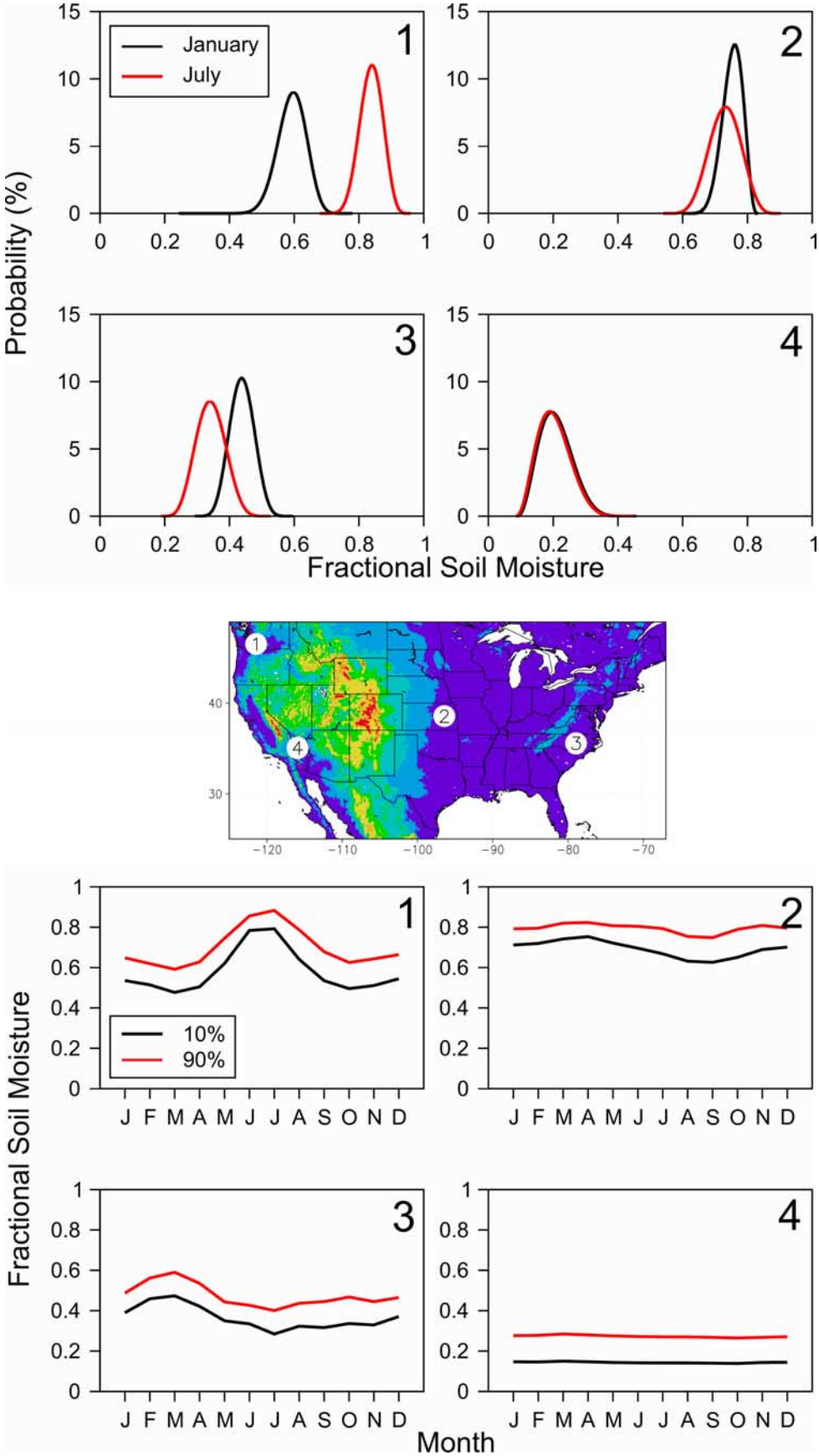

Figure 3

21562202d, 2004, D24, Downloaded from https://agupubs.onlinelibrary.wiley.com/doi/10.1029/2004JD005182, Wiley Online Library on [24/05/2023]. See the Terms and Conditions (https://onlinelibrary.wiley.com/terms-and-conditions) on Wiley Online Library for rules of use; OA articles are governed by the applicable Creative Commons License

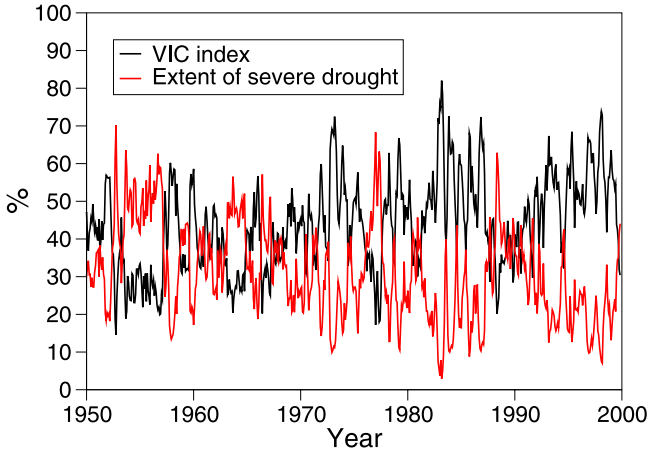

Figure 4. Time series of the monthly VIC drought index (%) averaged over the continental United States (black line) and areal extent of severe drought (red line) for 1950–1999. The areal extent is calculated as the percentage area of the continental United States for which the index is less than 10%.

distinct division between the long-term behavior in regions in the west and those in the east of the country. The most easterly regions (Ohio, Northeast, Middle Atlantic, Lower Mississippi, and Southeast) all exhibit quite similar variability and range of values. The rest of the country to the west exhibits less variability and much more persistence. *Diaz* [1983] analyzed statewide PDSI values for 1895–1981 and found a similar distinction between east and west, with frequently dry conditions west of the eastern Great Plains and wetter conditions to the east and especially in the southern Gulf Coast states. The level of persistence can be quantified by constructing a simple Markov chain for drought, with states $q(\theta) < 10\%$, $10\% <= q(\theta) <= 90\%$, and $q(\theta) > 90\%$, and calculating the monthly transition probabilities $P(q_{<10\%}, t) \rightarrow P(q_{<10\%}, t + 1)$. For the western RFC regions the average transition probabilities range from 0.74 for the North-Central to 0.86 for the Colorado Basin. For the eastern RFC regions, values range from 0.57 in the Mid-Atlantic to 0.61 in the Southeast region confirming the higher level of drought persistence in the west. Some degree of spatial coherence of long-term behavior is apparent between neighboring regions, as they experience similar climate conditions. For example, the California Nevada and Colorado Basin regions show similar behavior during the 1980s and 1990s, with less coherence before this time, although both tend to exhibit drier conditions. The Northeast and Middle Atlantic regions both show a slow descent into dry conditions in the early 1960s and then gradual recovery through the end of the decade. The Arkansas Red Basin and West Gulf regions exhibit high coherence in the earlier part of the time period, especially during the 1950s drought and the subsequent recovery into the 1960s, although severe drought conditions start earlier in the West Gulf region.

[26] Several periods of severe and extended drought can be identified and are consistent with the behavior at the national scale as seen in Figure 4. In 1988, in the North Central and Ohio River Basin, the average index drops to near zero in June and July, with a corresponding spatial coverage of nearly 100% below the 10% level. However, this only persists for a few months during the summer, after which the Ohio Basin wets up dramatically due to the return to more normal meteorological conditions [*Ropelewski*, 1988; *Namias*, 1991]. Also notable is the extensive and more persistent drought in the autumn and winter of 1976–77 in the North Central region, although the large-scale extent of this drought event in the West is restricted to one or two months duration. The early to mid 1960s in the Northeast and Middle Atlantic regions is also prominent, although this is masked to some extent by the large monthly variability. *Diaz* [1983] reported that this drought reached moderate to extreme levels over these two regions from mid-1964 to mid-1966 and this is reflected in the time series in Figure 5. Severe and persistent drought is evident during the mid 1950s in the Arkansas-Red Basin and West Gulf regions and to a lesser extent in the Colorado region. Note the sudden increase in values in the Arkansas-Red and West Gulf regions that occur in the early part of 1957, when spring rains alleviated the 1950s drought. In general, the western regions stand out as being more prone to the impacts of drought because of the higher level of persistence. The California, Nevada, and Colorado regions, especially, have experienced long-term, widespread drought for much of the period from the 1950s to the mid 1970s. At this point there is a switch to relatively drought free conditions for almost a decade, most notably in the Colorado Basin region, which may be related to Pacific decadal variability [*Barlow et al.*, 2001]. Drier conditions then tend to prevail through the mid-1980s to mid-1990s in these regions and in general across the northwest (including the Northwest and Missouri Basin regions). The climate in these regions is known to be impacted by the Pacific Decadal Oscillation (PDO) [*Barlow et al.*, 2001] which persists in a positive phase during this period.

4.4. Comparison With PDSI

4.4.1. National Scale

[27] In this section the VIC drought index is compared with three gridded PDSI data sets over the continental United States for the same 50-year period. Such a comparison is useful for evaluating the VIC index and its ability to identify drought occurrence and development. The PDSI is one of the most widespread used drought indices in the United States, although its use is decreasing, and was developed to measure the cumulative departure of moisture supply. The index is based on a simple water balance using a generic two-layer soil model and observed meteorology

Figure 3. Examples of the fitted distributions of monthly average fractional soil moisture VIC 50-year (1950–1999) retrospective simulation at four selected grid cells whose locations are given in the middle panel. The top panel shows probability distribution functions for January (black lines) and July (red lines) for each grid cell. The bottom panel shows monthly time series of the 10% (black lines) and 90% (red lines) quantiles of the distributions for each grid cell.

21562202d, 2004, D24, Downloaded from https://agupubs.onlinelibrary.wiley.com/doi/10.1029/2004JD005182, Wiley Online Library on [24/05/2023]. See the Terms and Conditions (https://onlinelibrary.wiley.com/terms-and-conditions) on Wiley Online Library for rules of use; OA articles are governed by the applicable Creative Commons License

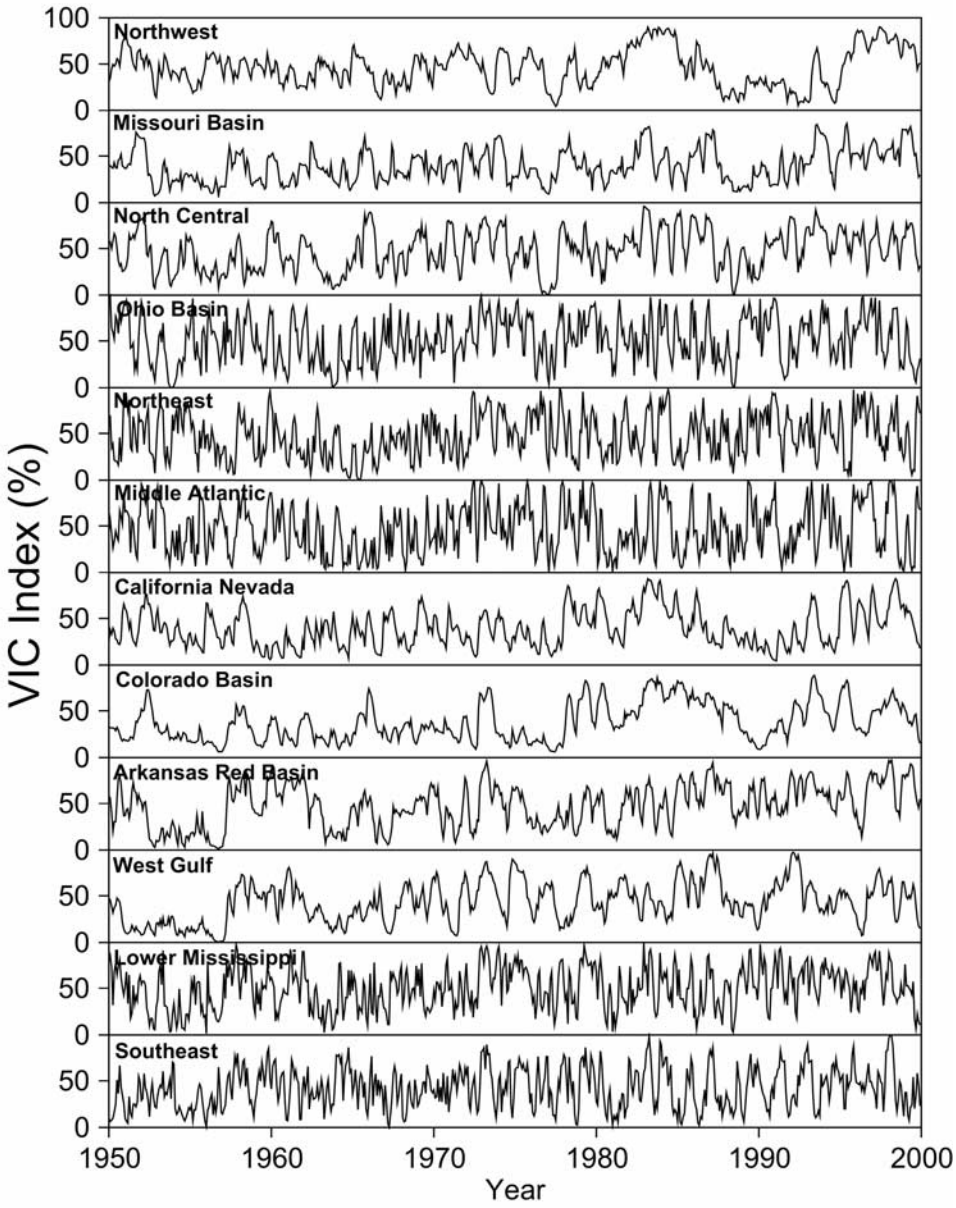

Figure 5. Time series of the monthly VIC drought index (%) averaged over each of the 12 continental NWS Regional Forecast Center regions for 1950–1999.

that is normalized with a reference set of water balance terms [*Palmer*, 1965]. The first comparison PDSI data set is the *Cook et al.* [1999] annual reconstruction of PDSI for the United States on a $2^\circ \times 3^\circ$ grid (referred to hereinafter as the Cook data set). The data set is derived using instrumental data over the last 100 years and tree ring data before that. The instrumental record is derived from the station based Historical Climatology Network (HCN) [*Karl et al.*, 1990], which was modified according to *Guttman* [1991]. The second comparison data set is the Dai PDSI [*Dai et al.*, 1998], which consists of monthly PDSI for global land areas on a $2.5^\circ \times 2.5^\circ$ grid for 1860 to 1995 (referred to hereinafter as the Dai data set). The data are derived using monthly surface air temperature from *Hansen and Lebedeff* [1987] and precipitation from *Dai et al.* [1997]. Soil moisture capacity is fixed to climatological maps from *Webb et al.* [1993]. The third PDSI data set (referred to hereinafter as $PDSI_{retro}$) is calculated with data from the VIC 50-year retrospective simulation, that is, monthly precipitation and air temperature, and available water capacity of the soil taken from the retrospective simulation soil parameter database [*Maurer et al.*, 2002]. This data set is therefore available on the same 1/8th degree grid as the VIC simulations and is driven by essentially the same forcings. The usual form of the PDSI algorithm uses a number of empirical constants to characterize the local climate. These were originally derived by Palmer using data from a number of climate divisions generally located in the Midwest and as such are not representative of the whole United States. Therefore one criticism of the index is that it is spatially inconsistent and direct comparisons between locations cannot be made [*Alley*, 1984]. To overcome this, a

21562202d, 2004, D24, Downloaded from https://agupubs.onlinelibrary.wiley.com/doi/10.1029/2004JD005182, Wiley Online Library on [24/05/2023]. See the Terms and Conditions (https://onlinelibrary.wiley.com/terms-and-conditions) on Wiley Online Library for rules of use; OA articles are governed by the applicable Creative Commons License

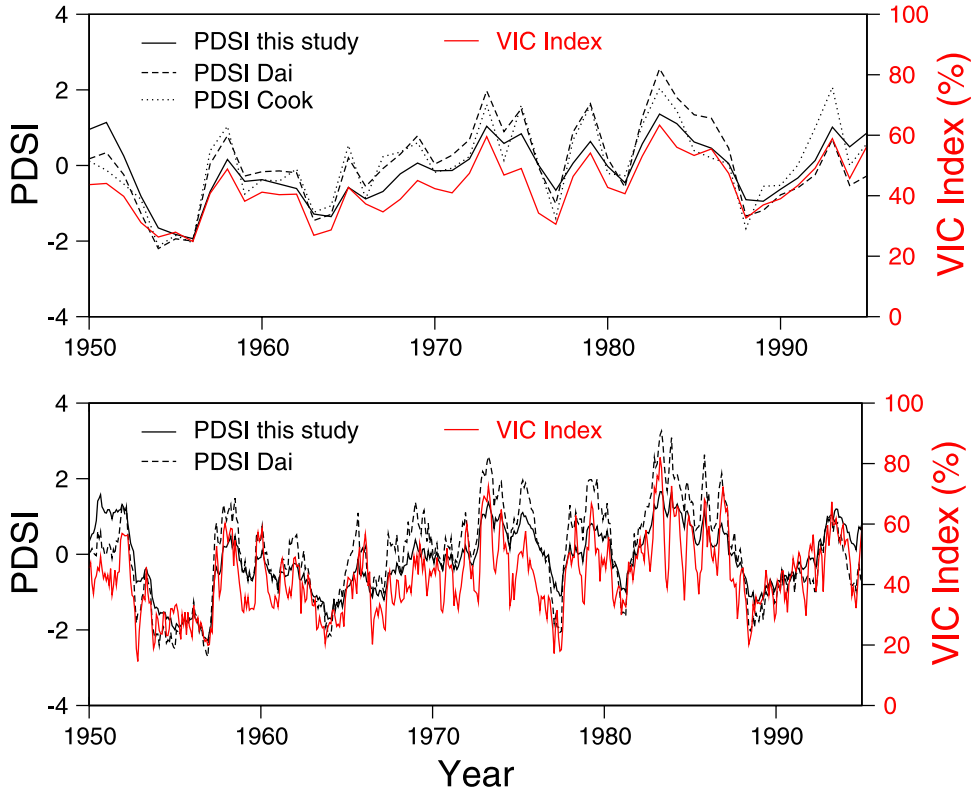

Figure 6. Comparison of time series of the VIC drought index for 1950–1995 averaged over the continental United States with three PDSI data sets. The top panel compares annual time series of the VIC index with (1) the PDSI derived using the VIC precipitation and temperature forcings ($PDSI_{retro}$), (2) the *Dai et al.* [1998] PDSI monthly data set, and (3) the *Cook et al.* [1999] reconstructed PDSI annual data set. The bottom panel compares monthly time series of the VIC index with (1) the $PDSI_{retro}$ data set and (2) the Dai data set.

self-calibrating version of the algorithm is used in which these constants are determined for each location using the time series of meteorology [*Wells et al.*, 2004].

[28] It is not expected that comparisons with the Cook and Dai PDSI data sets at smaller space scales will reveal high agreement because of the differences in resolution and data sources of the various data sets. To investigate the effect of resolution and whether the comparisons could be biased by the scaling properties of the PDSI, comparisons were carried out between a PDSI data set generated at 2.0 degree resolution (using the precipitation and temperature forcings aggregated up to 2.0 degree) and a data set generated at 1/8th degree, which was then aggregated up to 2.0 degree. The two data sets are highly correlated in the eastern part of the United States, but the correlation decreases as we move westward and is lowest, yet still significant, over the mountainous regions of the West, presumably because of the higher spatial variability of the precipitation and temperature inputs. At their worse, the differences between the data sets for individual months and seasons can manifest themselves as severe drought conditions in one data set and very wet conditions in the other. The implication is that the PDSI scales nonlinearly as a function of the spatial variability of the meteorological forcings and therefore caution should be exercised when interpreting the PDSI across various scales. However, while differences are apparent at small scales, these effects dissipate as we move to larger scales of averaging and are essentially negligible at the scale of the United States.

[29] In addition to these scaling issues, it is also important to note that the two types of index (PDSI and VIC drought index) are not directly comparable because of differences in definition and calculation. Nevertheless, it is useful to see how well the indices match over the large scale in terms of trends and variability and whether the VIC drought index can identify the major wet and dry spells over the last 50 years that are evident in the PDSI data sets. Figure 6 shows time series of indices averaged over the continental United States for the VIC based drought index and the three PDSI data sets. The comparison with the annual Cook data set reveals good agreement in the general year-to-year fluctuations and trends. This would be expected on an annual basis as drought is primarily driven by variability in precipitation and both data sets derive precipitation from the HCN, although they may use different subsets of stations and interpolation methods to grid the data. The comparison with the monthly PDSI data sets (Dai and $PDSI_{retro}$) reveals more interesting information on the performance of the VIC drought index. The Dai data set uses precipitation derived from the Global Historical Climatology Network, which, like the $PDSI_{retro}$ and Cook data sets, uses data from the U.S. HCN. Subsequently, the trends and major events are similar in the two data sets. However, the VIC index exhibits far greater variability in its values

215622024, 2004, D24, Downloaded from https://agupubs.onlinelibrary.wiley.com/doi/10.1029/2004JD005182, Wiley Online Library on [24/05/2023]. See the Terms and Conditions (https://onlinelibrary.wiley.com/terms-and-conditions) on Wiley Online Library for rules of use; OA articles are governed by the applicable Creative Commons License

that sometimes show large swings from wet to dry spells. This higher variability in the VIC index, or the lack of variability in the Dai data set, may be attributable to a number of factors, including most importantly the effect of spatial scale underlying the precipitation and meteorological data, and differences in the derivation and scaling of the two indices. However, known deficiencies in the application and underlying assumptions of the PDSI [*Guttman*, 1991; *Heim*, 2002; *Keyantash and Dracup*, 2002] point toward an underestimation of the variability. For example, the calculation of water balance terms over large time steps (monthly in the case of the Dai data set), the use of time invariant vegetative cover, and ignoring the effect of snowmelt, would all tend to dampen the evolution of the index over seasonal time scales.

4.4.2. Drought of 1988

[30] The drought of 1988 over the central United States is estimated to have cost $30 billion in agricultural losses alone and has been considered to be the worst natural disaster in U.S. history [*Trenberth and Branstator*, 1992]. It is generally agreed that a combination of sea surface temperature (SST) anomalies, persistent stationary atmospheric circulation and soil moisture-precipitation feedbacks were key factors in the development and longevity of the drought [*Sud et al.*, 2003]. Figure 7 shows a comparison of monthly maps of the VIC index with the $PDSI_{retro}$ data set during 1988. Although the two indices cannot be compared directly, the figure does reveal some interesting comparisons in the temporal and spatial evolution of the drought. The spring of 1988 was characterized by dry conditions over much of the western and midwestern United States [*Janowiak*, 1988], which is evident in the VIC index (not shown for the western United States). Interestingly, the PDSI does not show such extensive drought conditions in the West and has near-normal conditions ($-2.0 <$ PDSI < 2.0) over much of the Midwest. According to the VIC index, extensive drought conditions throughout the central United States were initiated during May. This coincides with changes to atmospheric circulation during April–June [*Trenberth and Branstator*, 1992], which led to below normal precipitation across the central Plains. The VIC index shows a lag of about 1 month to the changes in atmospheric conditions while the meteorological anomalies propagate through the soil column. For the PDSI, drought conditions appear first in the northern Plains in May and June, while the rest of the central United States remains in a fairly steady state. The maximum extent of negative precipitation anomalies occurred in June across a large region extending from the upper Midwest to the east coast [*Ropelewski*, 1988]. This is reflected in the VIC index which shows the maximum extent of drought during June with index values <10% over the majority of the region and is in stark contrast to the development and spatial extent of drought conditions from the PDSI. From May to June the PDSI begins a gradual descent into drier conditions across the central Plains as scattered regions of severe drought appear and the anomalous wet region extending down toward Texas recedes. Precipitation conditions returned to near normal conditions during July and August for large parts of the drought affected area, firstly in the east in July and then through the upper Midwest and much of the central and southern Plains in August [*Ropelewski*, 1988; *Namias*, 1991]. Despite the end of meteorological drought through July and August, record high surface air temperatures and accompanying significant evapotranspiration ensured that severe hydrological and agricultural drought conditions prevailed through the summer [*Trenberth and Branstator*, 1992]. Both the VIC index and PDSI reflect this and show persistent drought conditions across the central Plains through to the end of the year. Further coherence between the indices is evident across the lower Mississippi and Ohio River basins where they show a return to wetter conditions from September onward.

5. Discussion

5.1. Sources of Error

[31] The VIC drought index relies on modeling of soil moisture and is thus subject to errors that permeate the calculation of the data and the derivation of the index. In the absence of nationwide, long-term, consistent soil moisture observations at any scale, modeling is a useful alternative. Although validation studies have shown that the modeled data sets used here are reasonable in regions with available observational data [*Maurer et al.*, 2002; *Robock et al.*, 2003], it is undeniable that errors, albeit generally unquantifiable, are inherent in the data.

[32] In terms of readily identifiable errors, perhaps the most important are the meteorological forcings to the VIC land surface model. For example, the precipitation in the real-time data set is known to be biased in parts of the mountainous western United States, where grid estimates are based on gauges generally located in valley bottoms, which tend to be yield lower totals than the surrounding hills [*Pan et al.*, 2003]. Future versions of the real-time forcing data will hopefully address such errors [*Cosgrove et al.*, 2003]. Additionally, the assumed uniform diurnal precipitation rate (section 2.2) in the long-term retrospective simulation will result in incorrect model response in areas of infiltration limited runoff (Horton runoff), although the effect at the monthly scale of the drought index is unknown but presumably small. This potential problem does not apply to the near-term retrospective and real time simulations which use hourly precipitation and an hourly model time step.

[33] Errors are also inherent, but often much less apparent, in the physics and parameterizations of the land surface model, just as there are inaccuracies in the physical representations of the water balance models used in the calculation of standard drought indices. The VIC model attempts to simulate all aspects of the land surface water and heat budgets as accurately as possible, but in the end this is an estimate. Validation studies do show that the simulations of large-scale hydrologic variables are reasonable [e.g., *Maurer et al.*, 2002], although other studies indicate that there are areas of concern that will lead to errors in the soil moisture estimates. For example, comparison of the NLDAS near-term retrospective simulation (1996–1999) heat fluxes with observations from the Oklahoma ARM-CART observational network indicate that the VIC model underestimates evaporative fluxes [*Robock et al.*, 2003]. This may have associated effects on the accuracy of soil moisture estimates, although this is difficult to verify given that soil moisture mean and variability are unknown at any

15622024, 2004, D24, Downloaded from https://agupubs.onlinelibrary.wiley.com/doi/10.1029/2004JD005182, Wiley Online Library on [24/05/2023]. See the Terms and Conditions (https://onlinelibrary.wiley.com/terms-and-conditions) on Wiley Online Library for rules of use; OA articles are governed by the applicable Creative Commons License

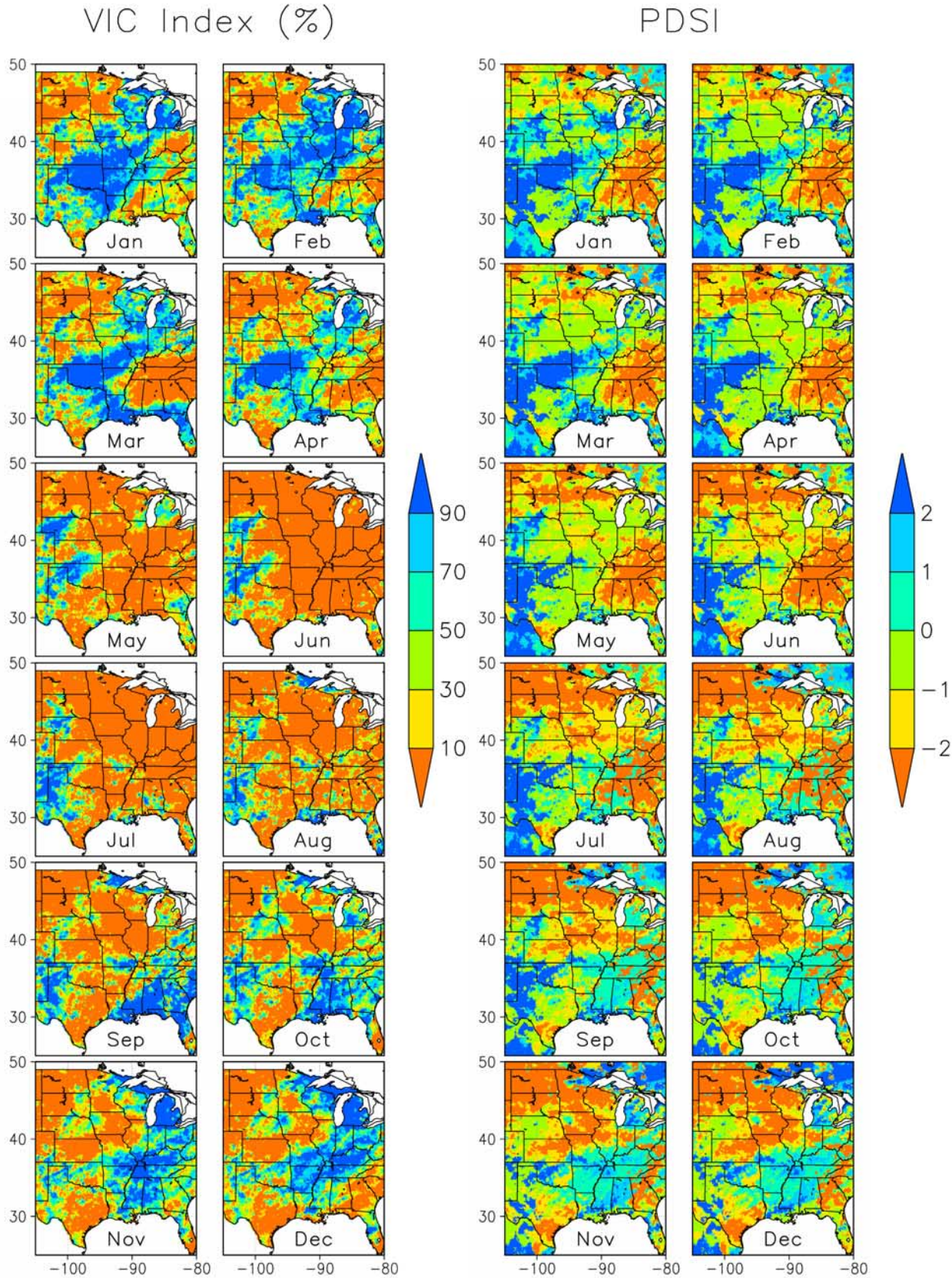

Figure 7

21562202d, 2004, D24, Downloaded from https://agupubs.onlinelibrary.wiley.com/doi/10.1029/2004JD005182, Wiley Online Library on [24/05/2023]. See the Terms and Conditions (https://onlinelibrary.wiley.com/terms-and-conditions) on Wiley Online Library for rules of use; OA articles are governed by the applicable Creative Commons License

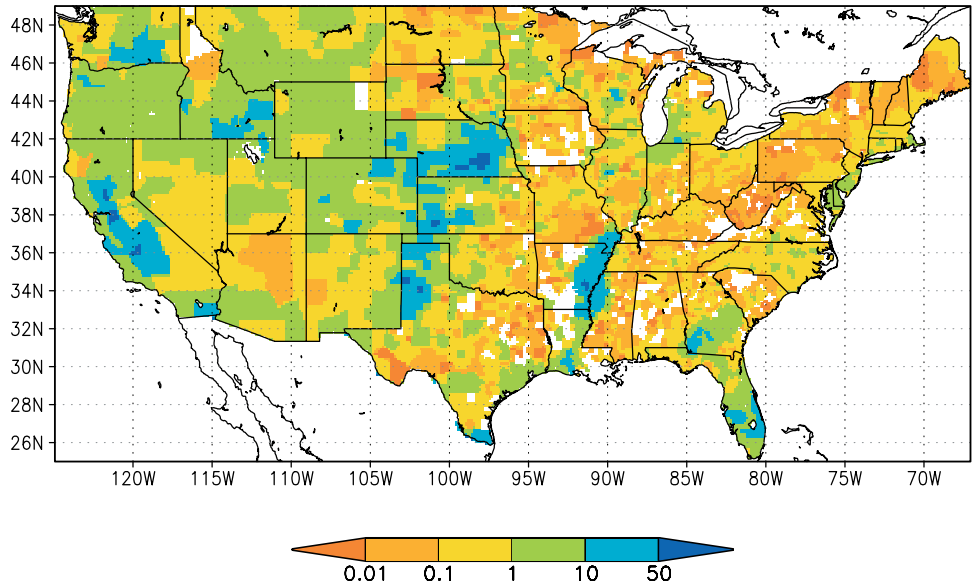

Figure 8. Percentage area equipped for irrigation in the United States in 1995 as derived from the 5-min global data set of *Siebert et al.* [2002] and averaged to the 1/8th degree grid of the VIC simulations. White colored areas have no available data. Blue colored regions have more than 10% fractional area equipped for irrigation, and the simulated soil moisture in these regions is potentially less reliable.

scale, making comparisons between different observational systems (point, areal via satellite, model) difficult.

[34] The fitted probability distributions contain some level of error due to the imperfect fit to the data. In the end the fit is a compromise whose level of error can be estimated using the K-S index or a mean square error. For extreme values of soil moisture, which are most pertinent for drought monitoring, the index is sensitive to small changes in values at the tails of the PDF. If the soil moisture data and the fitted PDFs are not representative, then the errors associated with quantifying drought may be high. It is assumed that the 50-year retrospective simulation, which is used as a baseline period for estimating the soil moisture climatology, is a representative sample and is long enough to encompass the annual variability in soil moisture. The results are heartening in that the calculations were done on 1/8th degree grids independently of other grids, yet spatial coherence is observed (see Figure 2) and hydrologic meaning can be attributed to the differences observed across the country.

[35] It is also assumed that the time period exhibits no significant trends that would render the climatology useless. Observational evidence based on gauge networks indicate that some regional changes may have occurred over the second half of the 20th century for precipitation [e.g., *Karl and Knight*, 1998] and streamflow [e.g., *Lins and Slack*, 1999] and especially in the West as manifested in reductions in snow accumulation and changes to spring snowmelt timing [*Mote*, 2003]. Whether such trends are evident in the VIC simulated data set is unclear and further analysis is required to assess any impacts on the calculation of drought indices. Furthermore, the influence of human activities is not accounted for explicitly in the modeling. This influence may be in terms of normal activities such as irrigation that directly affect soil moisture values, but may also consist of responses to drought conditions, such as land use changes. Figure 8 shows areas equipped for irrigation in the United States in 1995, as derived from the global data set of *Siebert et al.* [2002]. As the physical modeling does not take into account irrigation activity, the map indicates where the simulated soil moisture may potentially be less accurate, although this is dependent on actual irrigation and how irrigation practice has changed before 1995.

5.2. Identification of Different Drought Types

[36] The occurrence of drought can exist in a number of different forms depending on its impact [*Wilhite*, 2000]. Shortage of water in the near surface soil may indicate short-term meteorological drought but may not be a good measure of agricultural drought if the total root zone water storage is relatively wet. A long-term lack of water in the total soil column may be indicative of hydrological drought but a single storm may replenish root zone soil moisture enough to relieve agricultural drought, yet hydrological

Figure 7. Monthly VIC drought index and PDSI for 1988. For the VIC index, values toward the lower end of the scale (red colors) represent soil moisture values that are significantly lower than its long-term mean and can be said to be experiencing drought conditions. An index value toward 100% represents abnormally wet conditions (blue colors). PDSI values between −2 and 2 are classified as near normal conditions, values greater than 2 indicate wet conditions, and values less than 2 indicate drought conditions with values less than 4 being classified as extreme drought. The PDSI data were generated using the algorithm of *Wells et al.* [2004] on the same grid and using the same precipitation and temperature forcings as the VIC retrospective simulation.

21562202d, 2004, D24, Downloaded from https://agupubs.onlinelibrary.wiley.com/doi/10.1029/2004JD005182, Wiley Online Library on [24/05/2023]. See the Terms and Conditions (https://onlinelibrary.wiley.com/terms-and-conditions) on Wiley Online Library for rules of use; OA articles are governed by the applicable Creative Commons License

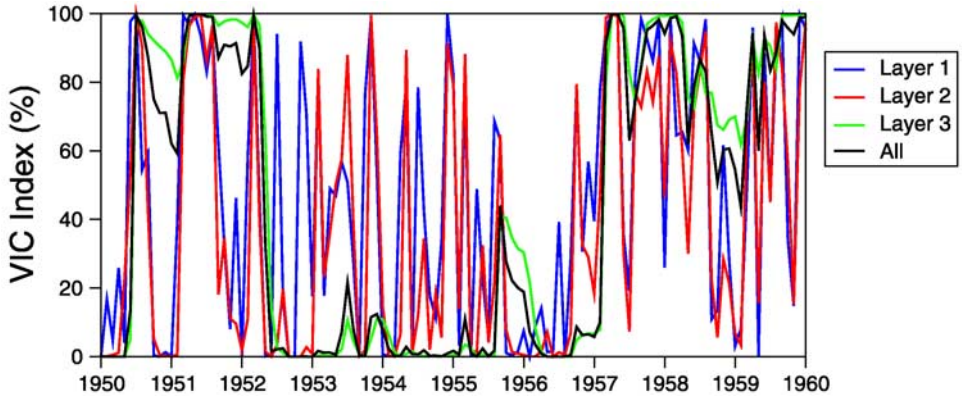

Figure 9. Time series of monthly VIC drought index (%) for the three model soil layers and the total soil column at a single grid cell in central Kansas (longitude −97.9375, latitude 38.5625) for 1950–1999. The thickness of the layers are as follows: top layer (1) = 0.1 m, middle layer (2) = 0.4 m, and bottom layer (3) = 0.5 m.

drought may still persist. With this kind of behavior in mind it is plausible that different drought types can be identified by examining the vertical distribution of moisture in the soil column. In addition to the total soil column moisture, data for three model sublayers are also available for the retrospective and real-time simulations. Therefore the drought index can be defined for different layers and combination of layers to represent different types of drought. For example, the near surface layer soil moisture may indicate the susceptibility to wild fire in that it gives a measure of the dryness of the overlying litter and brush. Deeper layers within the root zone represent the level of agricultural drought by quantifying the moisture available to root uptake. Deeper layers still are indicative of the available water for recharge to aquifers and baseflow to streams that may quantify the level of hydrological drought. Combinations of data from these different layers can be used to represent an overall index of drought, as shown previously for the total soil column.

[37] To illustrate this, Figure 9 shows the time series of drought index for the three model soil layers and the total soil column for 1950 to 1960 for a single grid cell in central Kansas. The period starts off generally wet, descends into drought conditions in the middle of the decade and then recovers to wetter conditions from 1957 onward. The top two soil layers show a close correlation and exhibit much greater variability than the lower layer, with regular switches between dry and wet conditions within the drier period of the middle of the decade. The deepest layer shows much more persistence than the top two layers, staying wet for the first three years, falling quickly into dry conditions and remaining persistently dry for several years until a sudden switch back to wet conditions in 1957. Of note is the different response in 1952, when the surface was dry but the deeper layer was wet, to that in 1953, when the deeper layer was very dry, but the surface was wet. These features reflect the general behavior of moisture over the vertical profile of the soil column, whereby near surface layers respond quickly to short term variations in precipitation, but deeper layers react in a dampened fashion and are guided by longer-term variations in climate. Although the drought index for the deep layer is quite persistent, it switches quickly between dry and wet conditions, leading to the possibility of preferred states in the soil moisture content at these lower depths (see *D'Odorico et al.* [2000] for a theoretical perspective). The drought index for the total soil column falls somewhere in between the values for the top two layers and the bottom layer, but is generally closer to the slowly developing lower layer as this index is dominated by the larger thickness of this deep layer. Such results highlight how the index can discern different drought conditions through the soil profile at the same time and how differently these conditions can develop and persist, illustrating the general difficulty in identifying and monitoring drought when specific impacts are of interest.

5.3. Importance of Cold Season Processes

[38] The importance of snow pack water storage in the mountainous West is well known and predicted to become critical in the near future due to regional warming [*Service*, 2004]. With up to 75% of all stream water being made up of snowmelt [*Service*, 2004], the role that cold season processes play in the development of summer drought and fire risk cannot be underestimated. The potential changes in climate on the timing of spring melt have great implications for drought development as well as for the risk of floods in the winter and spring. Modeling provides the benefit of being able to simulate cold season processes and explicitly model the development of the snow pack. As for soil moisture, the absence of large-scale measurements of snow water equivalent is problematic and ensures that modeling must play a central role in drought monitoring, amongst other hydrological studies. An example of the importance of cold season processes in drought monitoring is given in Figure 10, which shows the correlation between winter (DJF) snow water equivalent (SWE) and the summer (JJA) drought index. Very high correlation values indicate a strong relationship over much of the snow-affected parts of the United States and especially in the mountainous West, the northern Plains, and the northeast. This clearly shows the need to incorporate the effect of snow as a contributing factor in the development of drought.

[39] To illustrate this point further, Figure 11 shows the correlation for May between the VIC drought index and the

21562202d, 2004, D24, Downloaded from https://agupubs.onlinelibrary.wiley.com/doi/10.1029/2004JD005182, Wiley Online Library on [24/05/2023]. See the Terms and Conditions (https://onlinelibrary.wiley.com/terms-and-conditions) on Wiley Online Library for rules of use; OA articles are governed by the applicable Creative Commons License

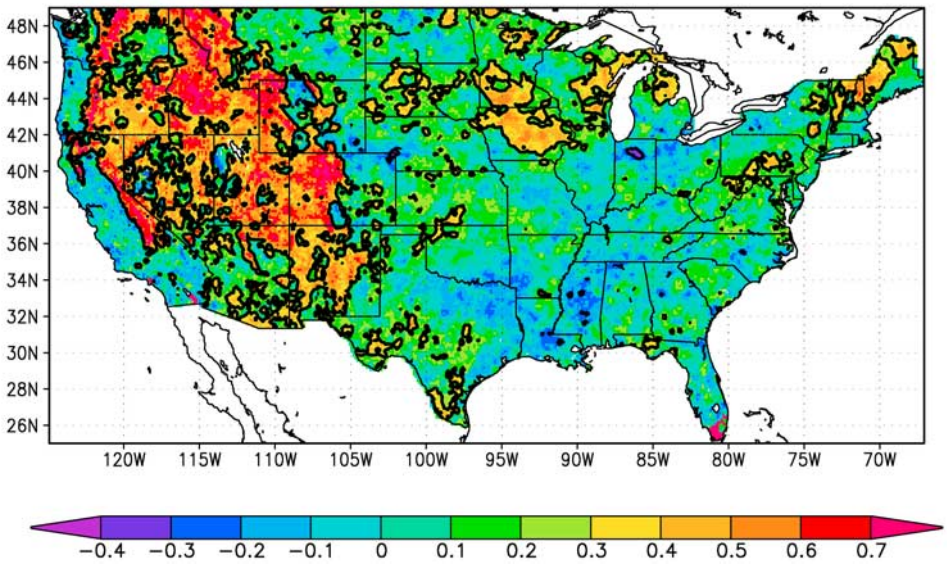

Figure 10. Correlation between wintertime (DJF) averaged VIC simulated snow water equivalent and subsequent summertime (JJA) averaged VIC drought index over the western United States. Contour lines indicate areas of significant local correlation at a 95% confidence level.

$PDSI_{retro}$ (see section 4.4), over the western United States, which covers the snow-dominated mountainous regions. Correlations are positive and significant at the 95% confidence level over the majority of the region indicating that the two indices are in general agreement, yet there are isolated areas that exhibit low or negative correlation. These areas generally coincide with regions of significant snow accumulation as shown in the map of springtime (MAM) average snow water equivalent derived from the retrospective simulation (Figure 11). The VIC retrospective simulation gives reasonable estimates of snow occurrence and accumulation (discussed in section 2.2; also see comparisons in *Pan et al.* [2003] and *Sheffield et al.* [2003]) and given the high correlation values elsewhere, it can be argued that the PDSI is likely in error over areas dominated by cold season processes. As the PDSI water balance model does not take into account the effects of frozen precipitation and snow accumulation, it tends to underestimate the occurrence of drought during winter and early spring and overestimate during the spring melt and summer. These areas of low and/or negative correlation do not exclusively correspond to areas of high snow accumulation. For example, northwest Utah and the southeast California desert also exhibit such correlation values but receive little, if any, precipitation and therefore the VIC index and the PDSI are likely to be more sensitive and will thus be dominated by the characteristics of their calculation methods rather than their inputs.

5.4. Drought Severity and Impacts

[40] The short analysis of drought occurrence presented here is based on an arbitrarily chosen threshold of 10% cumulative probability to represent severe drought conditions. This value was deemed as a reasonable threshold to describe dry conditions relative to the long-term mean. Other drought indices are often based on some probability distribution of a measured or calculated value and levels of drought are defined as intervals of this distribution [*Keyantash and Dracup*, 2002]. Often, the measured or calculated value is combined with some measure of persistence and threshold values for the onset and recession of drought. The index in this study is a raw measure of drought that estimates the current soil moisture values relative to the long-term mean, in this case on a monthly basis. As such it does not explicitly quantify the persistence of drought conditions and how these relate to the impacts. A month with extreme drought conditions may have little impact on, for example, water resources if the condition is relieved by subsequent rainfall, whereas a sequence of months of moderate drought may have more impact because of the cumulative effect. Such effects are complicated further by the timing of a drought in relation to demand, whether it is agricultural or human. This is an important area that will not be pursued in this study but is left for future work.

5.5. Real-Time Drought Monitoring and Forecasting

[41] The timely availability of information on drought conditions is central to the mitigation and alleviation of their adverse impacts. Soil moisture data are available from the NLDAS project in near real time (section 2.3) and provide the potential for implementing an operational drought monitoring index. The long temporal coverage of the 50-year historical simulation and the consistency with the real time simulation ensures that the system would possess the attributes necessary for operational monitoring [*Heim*, 2002]. Furthermore, there is potential for implementing the system in a forecast mode by using seasonal forecasts from coupled ocean-atmosphere general circulation models [*Wood et al.*, 2002].

6. Summary and Conclusions

[42] Soil moisture data from long-term retrospective simulations of the land surface water and energy budgets were used to construct probability distributions of monthly soil

21562202d, 2004, D24, Downloaded from https://agupubs.onlinelibrary.wiley.com/doi/10.1029/2004JD005182, Wiley Online Library on [24/05/2023]. See the Terms and Conditions (https://onlinelibrary.wiley.com/terms-and-conditions) on Wiley Online Library for rules of use; OA articles are governed by the applicable Creative Commons License

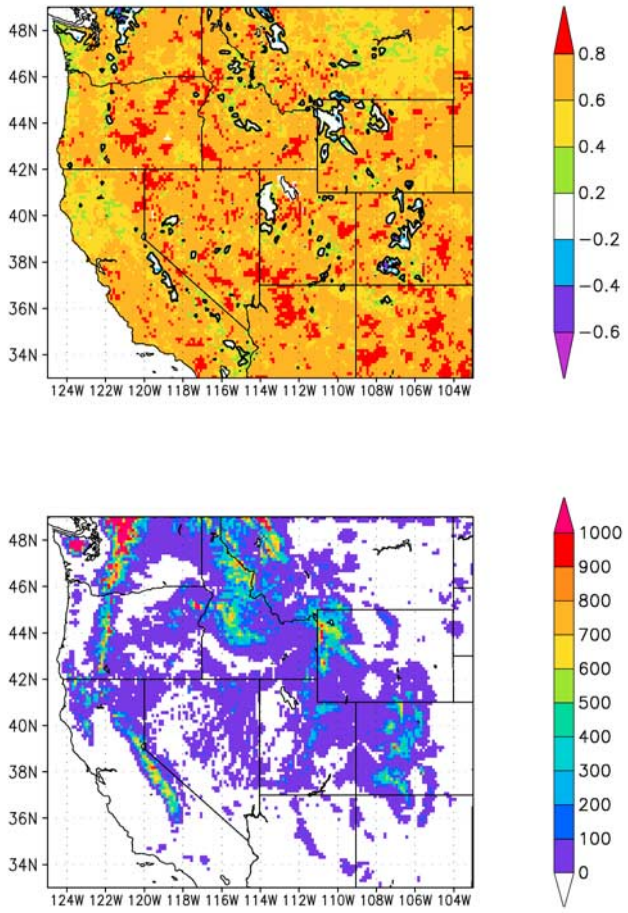

Figure 11. (top) Correlation between the VIC drought index and the PDSI derived using the VIC precipitation and temperature forcings ($PDSI_{retro}$) over the western United States for May. Areas of nonsignificant local correlation are shown in white, and the contours indicate local significance at a 95% confidence level. (bottom) Springtime (MAM) average snow water equivalent from the VIC 50-year (1950–1999) retrospective simulation.

moisture. The quantiles corresponding to the soil moisture of a particular month, within the fitted probability distributions, were used as a measure of drought. The analysis indicates that the drought index can identify major drought events and shows potential for implementation in an operational (and possibly forecast) mode. Further detailed analysis is required to reveal the accuracy and applicability of the index and to understand the complex processes involved in the development of drought in time and space. However, it is useful at this stage to highlight the main features of the index and how these instill confidence in the results, especially given the inherent difficulties in monitoring drought over large scales in a consistent fashion.

[43] 1. The index is based on simulations from a physical model, incorporating the full range of hydrological processes that contribute to the development and alleviation of drought. As well as modeling the full water and energy balance at the land surface, certain storages and processes not generally incorporated into other indices are taken into account. For example, the model simulates cold season processes to track the accumulation and melting of snow pack storage, which are major components of the hydrological regime in the western mountains.

[44] 2. The simulations are driven by observation-based forcings and distributed vegetation and soil parameters, which although they have their own set of errors, are consistent in time and space and arguably are the best estimate at present over such large scales.

[45] 3. Validation studies at various scales indicate that the soil moisture and related hydrologic variables are reasonably simulated (sections 2.2 and 2.3). Although there are known and unknown errors in all levels of the modeling process, the various comparisons reveal that the simulations provide a viable alternative to the absence of large scale and long-term observations of soil moisture.

[46] 4. The index is tangible in that it gives a measure of drought in terms of soil moisture, which has a physical meaning. The modeled soil moisture reveals the highly dynamic nature of precipitation and meteorology in the upper soil layers, reflects agricultural and vegetative vigor through the dynamics of the root zone layer, and includes the long-term memory of the prevailing climate in the deeper soil layers. Defining the index over different combinations of these soil layers, allows for monitoring of different types of drought. Other variables, which may be more suited to other drought monitoring applications, such as streamflow for hydrological drought, are available from these modeling efforts and can easily be incorporated into the drought index.

[47] 5. The index is defined at high spatial resolution of 1/8th degree (about 12 km) over the United States. This takes into account smaller scale processes, such as topographic effects and variability in soil characteristics that influence drought development and provides information at the local scale that is necessary to assess the impacts of drought.

[48] 6. The index is generated from high temporal resolution modeled soil moisture data enabling the index to be derived at a variety of temporal scales, from daily up to annually. Furthermore, the resolution can account for small timescale fluctuations in the forcings and response mechanisms. For example, the precipitation inputs include variations in the duration and intensity of storm events and not just amounts. This ensures that the index is able to resolve events where a single storm may alleviate a drought condition. Some existing indices have monitored changes in soil moisture but can be prone to biases due to their temporal resolution. For example, the Crop Moisture Index [*Palmer*, 1965] is calculated on a weekly basis and may not be able to take into account short-term storms that may alleviate a drought [*Keyantash and Dracup*, 2002].

[49] 7. The multidecade length of the historic retrospective period is able to capture a large range of variability in soil moisture values and thus provide a reasonable estimate of the long-term mean behavior. Future work will extend the index back in time to before the 1930s to capture the long-term drought conditions of the dust-bowl period.

[50] 8. The index is being generated in near real-time using meteorological inputs from gauge and satellite-based systems and numerical weather forecast schemes with the potential to be implemented in an operational mode.

[51] The drought index described in this study provides a physically based and consistent estimate of the state of

21562202d, 2004, D24, Downloaded from https://agupubs.onlinelibrary.wiley.com/doi/10.1029/2004JD005182, Wiley Online Library on [24/05/2023]. See the Terms and Conditions (https://onlinelibrary.wiley.com/terms-and-conditions) on Wiley Online Library for rules of use; OA articles are governed by the applicable Creative Commons License

drought on a monthly time scale at high resolution across the United States. The limited analysis presented here shows encouraging results and the potential for implementation into an operational drought-monitoring tool. The scope of this paper does not allow for the detailed analysis of the soil moisture data and the resulting drought index. However, this is ongoing work that will look in detail at the development and occurrence of drought and the relationships with forcing variables via local-scale processes and large-scale climate links, which a physically based modeling approach allows.

[52] **Acknowledgments.** We thank Steve Burgess and an anonymous reviewer for their comments and suggestions that helped to improve and clarify this study. This work was supported by NOAA grants NA86GP0248 and NA0303AR4310001 and NASA grant NAG5-9486. The VIC 50-year retrospective soil moisture data set was provided by the surface water modeling group at the University of Washington and was downloaded from their website at http://www.hydro.washington.edu. The Dai Palmer Drought Severity Index data were provided by the NOAA-CIRES Climate Diagnostics Center, from their website at http://www.cdc.noaa.gov/. The North American Drought Variability PDSI Reconstructions of *Cook et al.* [1999] were provided by the NOAA Paleoclimatology Program of the National Climatic Data Center and downloaded from the National Geophysical Data Center website at http://www.ngdc.noaa.gov/paleo/paleo.html.

References

Abdulla, F. A., D. P. Lettenmaier, E. F. Wood, and J. A. Smith (1996), Application of a macroscale hydrologic model to estimate the water balance of the Arkansas-Red river basin, *J. Geophys. Res.*, *101*(D3), 7449–7459.

Alley, W. M. (1984), The Palmer Drought Severity Index: Limitations and assumptions, *J. Clim. Appl. Meteorol.*, *23*, 1100–1109.

American Meteorological Society (1997) Meteorological drought, *Bull. Am. Meteorol. Soc.*, *78*(5), 847–849.

Augustine, J. A., J. J. DeLuisi, and C. N. Long (2000), SURFRAD—A national surface radiation budget network for atmospheric research, *Bull. Am. Meteorol. Soc.*, *81*, 2341–2358.

Barlow, M., S. Nigam, and E. H. Berbery (2001), ENSO, Pacific decadal variability, and U.S. precipitation, drought, and stream flow, *J. Clim.*, *14*, 2105–2128.

Brock, F. V., K. C. Crawford, R. L. Elliott, G. W. Cuperus, S. J. Stadler, H. L. Johnson, and M. D. Eilts (1995), The Oklahoma Mesonet: A technical overview, *J. Atmos. Oceanic Technol.*, *12*, 5–19.

Campbell, G. S. (1974), A simple method for determining unsaturated conductivity from moisture retention data, *Soil Sci.*, *117*, 311–314.

Capehart, W. J., and T. N. Carlson (1997), Decoupling of surface and near-surface soil water content: a remote sensing perspective, *Water Resour. Res.*, *33*(6), 1383–1395.

Cherkauer, K. A., L. C. Bowling, and D. P. Lettenmaier (2002), Variable Infiltration Capacity (VIC) cold land process model updates, *Global Planet. Change*, *38*, 151–159.

Cook, E. R., D. M. Meko, D. W. Stahle, and M. K. Cleaveland (1999), Drought reconstructions for the continental United States, *J. Clim.*, *12*(4), 1145–1162.

Cosgrove, B. A., et al. (2003), Real-time and retrospective forcing in the North American Land Data Assimilation System (NLDAS) project, *J. Geophys. Res.*, *108*(D22), 8842, doi:10.1029/2002JD003118.

Crook, A. G. (1977), SNOTEL—Monitoring climatic factors to predict water-supplies, *J. Soil Water Conserv.*, *32*(6), 294–295.

Dai, A., I. Fung, and A. D. Del Genio (1997), Surface observed global land precipitation variations during 1900–1988, *J. Clim.*, *10*, 2943–2962.

Dai, A., K. E. Trenberth, and T. Karl (1998), Global variations in droughts and wet spells: 1900–1995, *Geophys. Res. Lett.*, *25*, 3367–3370.

Diaz, H. (1983), Drought in the United States—Some aspects of major dry and wet periods in the contiguous United States, 1895–1981, *J. Clim. Appl. Meteorol.*, *22*, 3–16.

D'Odorico, P., L. Ridolfi, A. Porporato, and I. Rodriguez-Iturbe (2000), Preferential states of seasonal soil moisture: The impact of climate fluctuations, *Water Resour. Res.*, *36*(8), 2209–2220.

Dracup, J. A., K. S. Lee, and E. G. Paulson Jr. (1980), On the definition of droughts, *Water Resour. Res.*, *16*(2), 297–302.

Duan, Q., S. Sorooshian, and V. Gupta (1992), Effective and efficient global optimization for conceptual rainfall-runoff models, *Water Resour. Res.*, *28*(4), 1015–1031.

Duan, Q., V. K. Gupta, and S. Sorooshian (1993), A shuffled complex evolution approach for effective and efficient global minimization, *J. Optimization Theory Appl.*, *76*(3), 501–521.

Duan, Q., S. Sorooshian, and V. K. Gupta (1994), Optimal use of the SCE-UA global optimization method for calibrating watershed models, *J. Hydrol.*, *158*, 265–284.

Dumenil, L., and E. Todini (1992), A rainfall-runoff scheme for use in the Hamburg climate model, in *Advances in Theoretical Hydrology, A Tribute to James Dooge*, *Eur. Geophys. Soc. Ser. Hydrol. Sci.*, vol. 1, edited by P. O'Kane, Elsevier Sci., New York.

Entekhabi, D., I. Rodriguez-Iturbe, and F. Castelli (1996), Mutual interaction of soil moisture state and atmospheric processes, *J. Hydrol.*, *184*(1–2), 3–17.

Guttman, N. (1991), Sensitivity of the Palmer hydrologic drought index to temperature and precipitation departures from average conditions, *Water Res. Bull.*, *27*, 797–807.

Hansen, J., and S. Lebedeff (1987), Global trends of measured surface air temperature, *J. Geophys. Res.*, *92*, 13,345.

Heim, R. R., Jr. (2002), A review of twentieth century drought indices used in the United States, *Bull. Am. Meteorol. Soc.*, *83*(8), 1149–1165.

Hosking, J. R. M. (1990), L-moments: analysis and estimation of distributions using linear combinations of order statistics, *J. R. Stat. Soc.*, *52*(1), 105–124.

Janowiak, J. E. (1988), The global climate for March–May 1988: The end of the 1986–87 Pacific warm episode and the onset of wide-spread drought in the United States, *J. Clim.*, *1*, 1019–1040.

Karl, T. R., and W. R. Knight (1998), Secular trends of precipitation amount, frequency, and intensity in the United States, *Bull. Am. Meteorol. Soc.*, *79*, 231–241.

Karl, T. R., C. N. Williams Jr., and F. T. Quinlan (1990), United States Historical Climatology Network (HCN) serial temperature and precipitation data, *Environ. Sci. Div. Publ. 3404*, 371 pp., Carbon Dioxide Inf. Anal. Cent., Oak Ridge Natl. Lab., Oak Ridge, Tenn.

Keyantash, J., and J. A. Dracup (2002), The quantification of drought: An evaluation of drought indices, *Bull. Am. Meteorol. Soc.*, *83*(8), 1167–1180.

Kogan, F. N. (1997), Global drought watch from space, *Bull. Am. Meteorol. Soc.*, *78*(4), 621–636.

Koster, R. D., M. J. Suarez, R. W. Higgins, and H. M. Van den Dool (2003), Observational evidence that soil moisture variations affect precipitation, *Geophys. Res. Lett.*, *30*(5), 1241, doi:10.1029/2002GL016571.

Liang, X., D. P. Lettenmaier, E. F. Wood, and S. J. Burges (1994), A simple hydrologically based model of land surface water and energy fluxes for GSMs, *J. Geophys. Res.*, *99*(D7), 14,415–14,428.

Liang, X., E. F. Wood, and D. P. Lettenmaier (1996), Surface soil moisture parameterization of the VIC-2L model: Evaluation and modifications, *Global Planet. Change*, *13*, 195–206.

Lins, H. F., and J. R. Slack (1999), Streamflow trends in the United States, *Geophys. Res. Lett.*, *26*, 227–230.

Lyon, B., and R. Dole (1995), A diagnostic comparison of the 1980 and 1988 U.S. summer heat wave-droughts, *J. Clim.*, *8*, 1658–1676.

Maurer, E. P., G. M. O'Donnell, D. P. Lettenmaier, and J. O. Roads (2001), Evaluation of NCEP/NCAR reanalysis water and energy budgets using macroscale hydrologic simulations, in *Land Surface Hydrology, Meteorology, and Climate: Observations and Modeling*, *Water Sci. Appl. Ser.*, edited by V. Lakshmi, J. Albertson, and J. Schaake, pp. 137–158, AGU, Washington, D. C.

Maurer, E. P., A. W. Wood, J. C. Adam, D. P. Lettenmaier, and B. Nijssen (2002), A long-term hydrologically-based data set of land surface fluxes and states for the conterminous United States, *J. Clim.*, *15*, 3237–3251.

McKee, T. B., N. J. Doesken, and J. Kleist (1993), The relationship of drought frequency and duration to timescales, paper presented at 8th Conference on Applied Climatology, Anaheim, Calif., 17–22 Jan.

McKee, T. B., N. J. Doesken, and J. Kleist (1995), Drought monitoring with multiple timescales, paper presented at 9th Conference on Applied Climatology, Dallas, Tex., 15–20 Jan.

Mitchell, K., et al. (1999), The GCIP Land Data Assimilation System (LDAS) project—Now underway, *GEWEX News*, *9*(4), 7–11.

Mitchell, K., et al. (2000), The collaborative GCIP land data assimilation (LDAS) project and supportive NCEP uncoupled land-surface modeling initiatives, paper presented at 15th Conference on Hydrology, Am. Meteorol. Soc., Long Beach, Calif.

Mitchell, K., et al. (2004), The multi-institution North American Land Data Assimilation System (NLDAS) project: Utilizing multiple GCIP products and partners in a continental distributed hydrological modeling system, *J. Geophys. Res.*, *109*, D07S90, doi:10.1029/2003JD003823.

Mo, K., J. Zimmerman, E. Kalnay, and M. Kanamitsu (1991), A GCM study of the 1988 United States drought, *Mon. Weather Rev.*, *119*, 1512–1532.

21562202d, 2004, D24, Downloaded from https://agupubs.onlinelibrary.wiley.com/doi/10.1029/2004JD005182, Wiley Online Library on [24/05/2023]. See the Terms and Conditions (https://onlinelibrary.wiley.com/terms-and-conditions) on Wiley Online Library for rules of use; OA articles are governed by the applicable Creative Commons License

Mote, P. W. (2003), Trends in snow water equivalent in the Pacific Northwest and their climatic causes, *Geophys. Res. Lett.*, *30*(12), 1601, doi:10.1029/2003GL017258.

Namias, J. (1966), Nature and possible causes of the northeastern United States drought during 1962–65, *Mon. Weather Rev.*, *94*, 543–554.

Namias, J. (1967), Further studies of drought over northeastern United States, *Mon. Weather Rev.*, *95*, 497–508.

Namias, J. (1982), Anatomy of Great Plains protracted heat waves (especially the 1980 U.S. summer drought), *Mon. Weather Rev.*, *110*, 824–838.

Namias, J. (1991), Spring and summer 1988 drought over the contiguous United States—Causes and prediction, *J. Clim.*, *4*, 54–65.

Nijssen, B., D. P. Lettenmaier, X. Liang, S. W. Wetzel, and E. F. Wood (1997), Streamflow simulation for continental-scale river basins, *Water Resour. Res.*, *33*(4), 711–724.

Nijssen, B., G. M. O'Donnell, D. P. Lettenmaier, D. Lohmann, and E. F. Wood (2001), Predicting the discharge of global rivers, *J. Clim.*, *14*, 3307–3323.

Palmer, W. (1965), Meteorological drought, *Res. Pap. 45*, 58 pp., U.S. Dep. of Commerce, Washington, D. C.

Pan, M., et al. (2003), Snow process modeling in the North American Land Data Assimilation System (NLDAS): 2. Evaluation of model simulated snow water equivalent, *J. Geophys. Res.*, *108*(D22), 8850, doi:10.1029/2003JD003994.

Piechota, T. C., and J. A. Dracup (1996), Drought and regional hydrologic variation in the United States: Associations with the El Nino-Southern Oscillation, *Water Resour. Res.*, *32*(5), 1359–1373.

Rajagopalan, B., E. Cook, U. Lall, and B. K. Ray (2000), Spatiotemporal variability of ENSO and SST teleconnections to summer drought over the United States during the twentieth century, *J. Clim.*, *13*, 4244–4255.

Rasmussen, E. M., R. E. Dickinson, J. E. Kutzbach, and M. K. Cleaveland (1993), Climatology, in *Handbook of Hydrology*, edited by D. R. Maidment, pp. 2.1–2.44, McGraw-Hill, New York.

Robock, A., et al. (2003), Evaluation of the North American Land Data Assimilation System over the Southern Great Plains during the warm season, *J. Geophys. Res.*, *108*(D22), 8846, doi:10.1029/2002JD003245.

Ropelewski, C. F. (1988), The global climate for June–August 1988: A swing to the positive phase of the southern oscillation, drought in the United States, and abundant rain in monsoon areas, *J. Clim.*, *1*, 1153–1174.

Schubert, S., M. Suarez, P. Pegion, R. Koster, and J. Bacmeister (2004), On the cause of the 1930s Dust Bowl, *Science*, *303*, 1855–1859.

Service, R. F. (2004), As the West goes dry, *Science*, *303*, 1124–1127.

Sheffield, J., et al. (2003), Snow process modeling in the North American Land Data Assimilation System (NLDAS): 1. Evaluation of model simulated snow cover extent, *J. Geophys. Res.*, *108*(D22), 8849, doi:10.1029/2002JD003274.

Siebert, S., P. Döll, and J. Hoogeveen (2002), Global map of irrigated areas version 2.1, Cent. for Environ. Syst. Res., Univ. of Kassel, Kassel, Germany.

Stedinger, J. R., R. M. Vogel, and E. Foufoula-Georgiou (1993), Frequency analysis of extreme events, in *Handbook of Hydrology*, edited by D. R. Maidment, pp. 18.1–18.66, McGraw-Hill, New York.

Sud, Y. C., D. M. Mocko, K.-M. Lau, and R. Atlas (2003), Simulating the Midwestern U.S. drought of 1988 with a GCM, *J. Clim.*, *16*, 3946–3965.

Svoboda, M., et al. (2002), The Drought Monitor, *Bull. Am. Meteorol. Soc.*, *83*(8), 1181–1190.

Trenberth, K., and G. Branstator (1992), Issues in establishing causes of the 1988 drought over N. America, *J. Clim.*, *5*, 159–172.

Webb, R. S., C. E. Rosenzweig, and E. R. Levine (1993), Specifying land surface characteristics in general circulation models: Soil profile data set and derived water-holding capacities, *Global Biogeochem. Cycles*, *7*, 97–108.

Wells, N., S. Goddard, and M. J. Hayes (2004), A self-calibrating Palmer drought severity index, *J. Clim.*, *17*, 2335–2351.

Wilhite, D. A. (2000), Drought as a natural hazard: Concepts and definitions, in *Drought: A Global Assessment*, edited by D. A. Wilhite, pp. 3–18, Routledge, London.

Wood, A. W., E. P. Maurer, A. Kumar, and D. P. Lettenmaier (2002), Long-range experimental hydrologic forecasting for the eastern United States, *J. Geophys. Res.*, *107*(D20), 4429, doi:10.1029/2001JD000659.

G. Goteti, Department of Earth System Science, University of California, Irvine, CA 92697, USA.

J. Sheffield and E. F. Wood, Department of Civil and Environmental Engineering, Princeton University, Princeton, NJ 08544, USA. (justin@princeton.edu)

F. Wen, Department of Mathematics, New York University, New York, NY 10003, USA.

21562202d, 2004, D24, Downloaded from https://agupubs.onlinelibrary.wiley.com/doi/10.1029/2004JD005182, Wiley Online Library on [24/05/2023]. See the Terms and Conditions (https://onlinelibrary.wiley.com/terms-and-conditions) on Wiley Online Library for rules of use; OA articles are governed by the applicable Creative Commons License